IMPROVING THE REPRESENTATION OF MULTICOMPONENT AEROSOLS IN NUMERICAL MODELS

By

Jin Lu

Dissertation
Submitted to the Vanderbilt University
in partial fulfillment of the requirements
for the degree of
DOCTOR OF PHILOSOPHY
in
Chemical Engineering
December, 2005
Nashville, Tennessee

Approved:
Frank M. Bowman
M. Douglas LeVan
Karl B. Schnelle, Jr.
G. Kane Kennings
Eugene J. LeBoeuf

To my mom and dad, Min Liu and BaoQuan Lu

my beloved wife, Ting Wang

my newborn son, Kevin Lu

for

their countless love

ACKNOWLEDGEMENTS

First, I would like to thank Dr. Frank M. Bowman for being a wonderful advisor. He led me into this exciting field, and always has been there to provide guidance and professional support. I greatly appreciate his enthusiasm and encouragement along my doctorial research. Dr. Bowman is also an excellent mentor, I have learned a lot from him, not only about research, but also about being a good person.

I also want to thank all the members in my advisory committee, Dr. M. Douglas LeVan, Dr. Karl Schnelle, Dr. G. Kane Jennings, and Dr. Eugene J. LeBoeuf, for their valuable comments and suggestions for my research and dissertation.

I would also like to thank the Department of Chemical Engineering at Vanderbilt University for its support during my graduate studies at Vanderbilt. Special thanks to Ms. Margarita Talavera for her kind help to me and my family.

I would like to express my deep gratitude to my parents, Min Liu and BaoQuan Lu, for their unconditional love and understanding throughout my lengthy career as a student.

Finally, I would like to thank my lovely wife, Ting Wang. Her love and support has been a constant source of hope and inspiration. Kevin, my dear newborn son, is the most precious gift for my graduation.

TABLE OF CONTENTS

Page

Chapter

LIST OF TABLES

LIST OF FIGURES

LIST OF SYMBOLS

Chapter II

A_i	mass concentrations of semivolatile species i in the gas phases ($\mu g\ m^{-3}$)
$C_{i,\infty}$	concentration of i in the bulk gas phase ($\mu g\ m^{-3}$)
$C_{s,i}$	gas-phase concentration of i in equilibrium with the aerosol particle ($\mu g\ m^{-3}$)
D_i	diffusivity of species i ($cm^2\ s^{-1}$)
D_p	particle diameter (μm)
F_i	mass concentrations of semivolatile species i in the particle phases ($\mu g\ m^{-3}$)
K_i	partitioning coefficient ($m^2\ \mu g^{-1}$)
M_o	concentration of absorbing aerosol ($\mu g\ m^{-3}$)
MW	mean molecular weight of aerosol phase ($g\ mol^{-1}$)
p_i^0	vapor pressure of compound i as a liquid (kPa)
R	gas constant ($=8.314\ J\ mol^{-1}\ K^{-1}$)
S_i	semivolatile organic
T	temperature (K)
α_i	mass stoichiometric coefficient of semivolatile organic
	accommodation coefficient of species i on the particle
λ	air mean free path (μm)
ζ_i	activity coefficient of compound i in aerosol phase

Chapter III

d_p	particle diameter (μm)
d_{pk}	median diameter of mode k (μm)
$d_{p(j-1)}$	lower size boundary of section j (μm)
d_{pj}	upper size boundary of section j (μm)
M_{ij}	mass of component i in section j (μg m^{-3})
NC	total number of components
NM	total number of modes in modal distribution
NS	total number of sections in sectional distribution
$q(d_p)$	aerosol mass size distribution function (μg m^{-3})
$q_i(d_p)$	mass size distribution of component i (μg m^{-3})
$q_k(d_p)$	mass size distribution of mode k (μg m^{-3})
Q_{ik}	mass of component i in mode k (μg m^{-3})
Q_{ik}'	mass of component i from mode k within sectional size boundaries (μg m^{-3})
Q_k	total mass in mode k (μg m^{-3})
T_{ijk}	mass of component i in section j from mode k (μg m^{-3})
T_{jk}	mass in section j from mode k (μg m^{-3})
x_{ij}	mass fraction of component i in section j
x_{ik}	mass fraction of component i in mode k
σ_k	standard deviation of mode k

Subscripts:

i	component number, 1 to NC
j	section number, 1 to NS
k	mode number, 1 to NM

Chapter IV

c	mixing threshold criterion
C_i	mass concentrations of semivolatile species i in the gas phases (μg m^{-3})
$C_{i,eq}$	gas-phase concentration in equilibrium with the aerosol particle (μg m^{-3})
$C_{i,\infty}$	concentration of i in the bulk gas phase (μg m^{-3})
D_i	diffusivity of species i (cm^2 s^{-1})
D_p	particle diameter (μm)
$f(i)$	binary number (0 or 1)
$f(i,j,k)$	volume fraction of coagulated particle to section k because of the coagulation of two particles from section i and j
F_i	mass concentrations of semivolatile species i in the particle phases (μg m^{-3})
H_i	enthalpy of vaporization of component i (kJ)
J_i	mass i transfer flux between gas and particle phase (μg s^{-1})
K_i	partitioning coefficient (m^2 μg^{-1})
m	index number of each particle population’s distribution
M_o	concentration of absorbing aerosol (μg m^{-3})
MW	mean molecular weight of aerosol phase (g mol^{-1})

$n^t(k)$	time-dependent number concentration of particle in section k at time t (# m^{-3})
N_c	total number of particle phase components
N_d	total number of aerosol distributions
N_Q	total number of components
N_S	total number of sections
N_T	total number of distribution
p_i^0	vapor pressure of compound i as a liquid (kPa)
R	gas constant (=8.314 J mol^{-1} K^{-1})
s_{ji}	number of functional groups of type j in each molecule i
T	temperature (K)
u_k	characteristic volume of particles in section k (μm^3)
$v^t_q(k)$	time-dependent volume concentration of component q of particle in section k at time t (μm^3 m^{-3})
r_a	aerodynamic resistance (s m^{-1})
r_b	quasi-laminar resistance (s m^{-1})
v_d	particle deposition velocity (m s^{-1})
v_s	particle gravitational settling velocity (m s^{-1})
α_i	accommodation coefficient of species i on the particle
β	coagulation kernel, or collision rate, of two colliding particles (cm^3 s^{-1})
λ	air mean free path (μm)
ζ_i	activity coefficient of compound i in aerosol phase

Subscripts:

i	component number, 1 to N_c
j	section number, 1 to N_S
k	distribution number, 1 to N_T

CHAPTER I

INTRODUCTION

Aerosols are small solid or liquid particles suspended in the gas. Atmospheric aerosol size ranges from a few nanometers (nm) to tens of micrometers (µm) in diameter. Hundred of chemical components have been found in atmospheric aerosols, such as sulfates, nitrates, ammonium, crustal material, water, alkanes, alkenes, PAH, and so on. Atmospheric aerosols are emitted from either natural sources, such as sea spray and road dust, or anthropogenic sources, such as cooking and fuel combustion. Aerosol particles emitted from different sources may have different composition and size distribution. Atmospheric aerosols contribute to a variety of air pollution problems, including adverse health effects (Phalen 1998; Pope 2000), visibility reduction (Blando et al. 1998; Malm et al. 2003), and global climate change (Penner et al. 2001). With their properties being further understood, atmospheric aerosols obtained more concern in recent years. Limited by the method and technology of measuring and the inherent properties of aerosol particles, it is impossible to identify and characterize all the atmospheric aerosols in an area, especially within a large scale. Therefore, numerical modeling method is developed and becomes a useful tool for predicting the properties of atmospheric aerosols (Jacobson 1997c; Seinfeld and Pandis 1998).

The overall objective of my research has been to improve the representation of multicomponent aerosols in numerical models. This research has focused on two main areas. One is to find a new method for converting multicomponent aerosol distributions from sectional to modal representation, and another is to investigate the interactions between aerosol mixing state, secondary organic aerosol partitioning, and coagulation.

The dissertation is organized as follows. Chapter II describes the background and significance of my research in detail. Chapter III defines the relationship between sectional and modal representations of multicomponent aerosol distributions, presents and evaluates a new conversion method to convert multicomponent aerosol distributions from sectional to modal representations using non-linear least square regression approach, and compares the conversion results with other conversion methods. Chapter IV defines a new sectional approach to represent size and compositionally resolved external aerosol mixtures, develops aerosol module incorporating sectional mixing state definition with new routines for coagulation, gas-particle partitioning, emission and deposition, and investigates the relationship between mixing state, SOA partitioning, and coagulation. Chapter V summarizes the results of these studies, gives overall conclusions, and provides suggestions and directions for future work.

CHAPTER II

BACKGROUND

Atmospheric Aerosols

Aerosols are fine solid or liquid particles suspended in the gas (Seinfeld and Pandis 1998). The diameter of atmospheric particles varies over 6 to 7 orders of magnitude and ranges from a few nanometers (nm) to tens of micrometers (μm). Two kinds of sources contribute to aerosols in the atmosphere: natural, such as sea spray, road dust, volcanic emission, biomass emission, etc., and anthropogenic, for example the particles emitted from fuel combustion and industrial processes. Based on the methods of formation, atmospheric aerosols can also be classified as primary aerosol, which is emitted directly from sources, and secondary aerosol, which is formed in the atmosphere by gas-to-particle conversion processes.

Atmospheric aerosols contribute to a variety of air pollution problems including adverse health effects, visibility reduction, and global climate change. Though there is still uncertainty about the specific physiological mechanisms leading to observed health effects, the fact that the aerosol indeed affects our health is clear (Phalen 1998; Pope 2000). Secondary aerosol formation from both natural and anthropogenic sources contributes to visibility degradation in national parks (Blando et al. 1998; Malm and Day 2000; Malm et al. 2003). Anthropogenic aerosol emissions affect the global radiative balance directly by scattering incoming sunlight and indirectly by modifying cloud droplet properties (Penner et al. 2001). Aerosol particles are also connected with many natural phenomena, such as the enhanced transportation of nonvolatile materials from one place to another.

Aerosol distributions and composition

Ambient air contains thousands to millions of particles floating in every cubic meter of air, each with its own size and composition. An idealized schematic in Figure 2.1 can be used to represent the size distribution of these particles. As shown in Figure 2.1, aerosol particles can be separated into a "coarse" mode (diameter > 2.5μm) and a "fine" mode (diameter < 2.5μm). Fine particles can be further classified into a nuclei mode (diameter < 0.1μm) and an accumulation mode (0.1μm < diameter < 2.5μm).

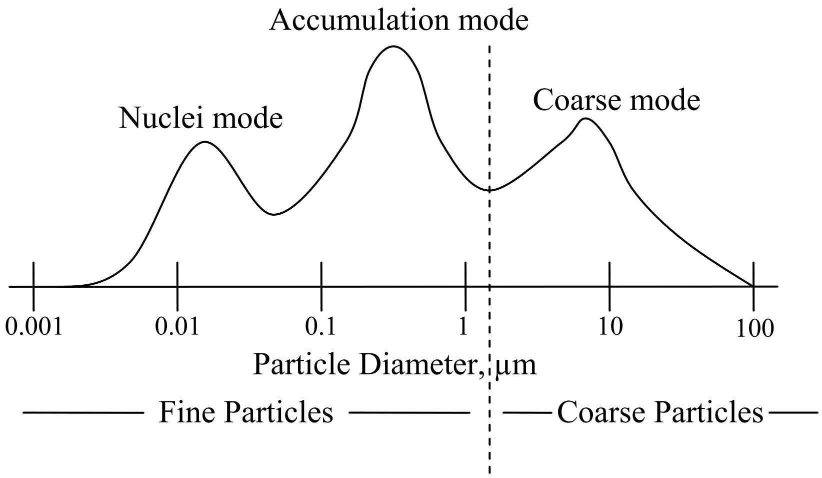

Figure 2.1 An idealized schematic of aerosol size distribution.

The composition of particles is extremely complex and varied. Hundreds of different chemical components have been detected in particle phase, including both inorganics, such as sulfate, nitrate, water, crustal materials, trace metals, etc, and organic materials, such as alkanes, alkenes, PAHs, and aromatic acids. Some of them are emitted directly from emission sources in particle phase. Others are emitted originally in gas phase and then condense to particle phase directly or after undergoing photochemical reactions that form new compounds with lower vapor pressure. Since chemical reactions may happen within the particle phase, and there are always particle-to-particle and particle-to-gas interactions, the composition of particles changes with time and location. Therefore, it is extremely difficult to completely characterize an aerosol particle.

The composition of aerosol varies with particle size. The formation of fine particles are mainly from chemical reactions and aerosol dynamic processes, so sulfate, ammonium, elemental and organic carbon, and trace metals are found predominantly in fine particles. Coarse particles mostly come from mechanical disposal and road dust, so crustal materials, such as silicon, calcium, and magnesium, and biogenic organic particles are usually in the coarse aerosol fraction (Seinfeld and Pandis 1998; Brasseur et al. 1999).

Aerosol processes

Once airborne, particles will interact with the surrounding multicomponent gas phase and other particles. Figure 2.2 shows the main aerosol processes occurring within a typical air parcel. The dynamic processes in this aerosol system are condensation, evaporation, coagulation, nucleation, advection, emission and deposition.

Coagulation occurs when particles stick together after collision with each other. The most important characteristics of coagulation are the increase of average particle size and the decrease of total particle number in the atmosphere. It does not substantially alter the volume of the large particles, but has a significant effect on the number size distribution of small particles (Lee 1983; Seigneur 2001).

Condensation is a gas-to-particle mass transfer process, where gas-phase components condense onto existing particles. *Evaporation* is the reverse mass transfer process of condensation, and aerosol components evaporate to gas phase. The predominant feature of the condensation/evaporation process is the increase/decrease of particle volume (or mass) with no change in number of particles.

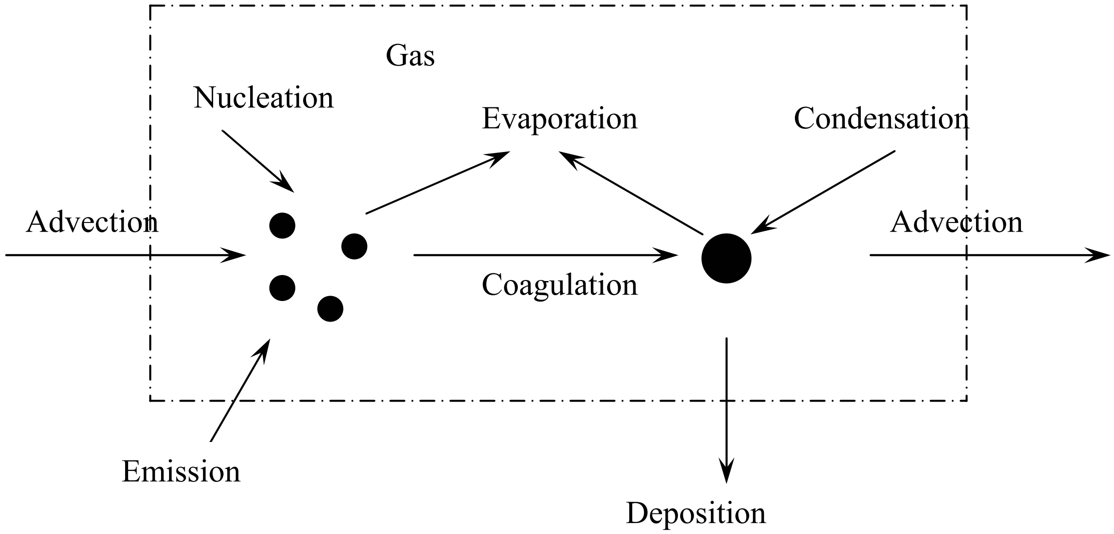

Figure 2.2 Representation of aerosol dynamics processes.

In *nucleation*, a large number of tiny particles are formed directly from supersaturated vapor. It is a very quick process that is very difficult to measure or simulate accurately because as soon as particles are formed they begin to grow via condensation and coagulation. So, in typical urban scale models, nucleation is either ignored or combined with condensation instead of a self contained process (Seigneur 2001; Griffin et al. 2002a).

Advection is the movement of particles by air flow. Because of advection and diffusion of particles, aerosols can be transferred from place to place and mixed with other kind of particles. *Emission* is the process that introduces primary particles into the atmosphere. The particles emitted from different sources may have different size and composition distribution. *Deposition* occurs when particle is captured by surface, and is the only way to remove aerosol from atmosphere. It can be classified as either dry deposition, where the aerosol particles deposit to surface without precipitation, or wet deposition, where the particles are washed out by rain or other large droplets (Seinfeld and Pandis 1998).

All of the above processes work together to affect the aerosol size distribution simultaneously. If all the dynamic processes are included in the definition of aerosol size distribution function, this is called the General Dynamic Equation (GDE) (Gelbard et al. 1980; Seinfeld and Pandis 1998).

Atmospheric models

In order to predict the ambient level of aerosol particles, three-dimensional air quality models of aerosol have been developed, which contains aerosol dynamic processes, interactions between gas and particle phase, gas phase chemistry, and so on (Binkowski and Shankar 1995; Jacobson 1997a; Kleeman et al. 1997; Lurmann et al. 1997; Ackermann et al. 1998; Meng et al. 1998; Sun and Wexler 1998a; Pilinis et al. 2000; Jacobson 2001a; Kleeman and Cass 2001; Binkowski and Roselle 2003).

The CIT model (Meng et al. 1998) is a typical 3-dimensional size-resolved and chemically resolved Eulerian aerosol model for urban scale simulation, where the aerosol particles are represented by fixed sectional distribution. When particles are treated as external mixture, the model is updated to CIT/UCD model (Kleeman et al. 1997; Kleeman and Cass 2001), where the emission of particles is separated to 10 different sources, including paved road dust, diesel engine, food cooking and sea spray. GATOR is another Eulerian aerosol model (Jacobson 1997a, 2001a), which can be used for a large scale and long time range simulation, where moving center sectional distribution is used to represent the distribution of aerosol particles and coagulation process is well treated. Models-3/CMAQ is another type of aerosol model (Binkowski and Shankar 1995; Binkowski and Roselle 2003), where the distribution of aerosol particles is represented by 3 lognormal modes. Because of the fast computation speed, Models-3/CMAQ is often used for regional scale and long term simulation. MADE is another model developed on modal aerosol distribution, where a sulfate-nitrate-ammonium-water system is constructed and a regional scale simulation on Europe is performed (Ackermann et al. 1998).

Based on the purpose of model construction, different models treat aerosol processes differently. There is a tradeoff between the level of detail and the simulation time needed due to computation cost associated with the numerical integration of the chemical dynamic equations. When a detailed treatment of aerosol processes is included, such as CIT and CIT/UCD, the application of these models is limited to only a few days of simulation. With simplified atmospheric chemistry system, the model can be used for a long term and large scale simulation, but the performance of simulation can not be guaranteed (Venkatram et al. 1997). For example, the global climate models can be used for 100 years simulation, where there is a very simplified description of aerosol particles, but the simulation results can only be an approximation.

Aerosol size distribution methods

Accurate and proper representation of aerosol size distribution is necessary for the application of an air quality model. Two of the most common approaches for describing aerosol size distributions are sectional and modal methods. Both have been widely used in atmospheric models (Warren and Seinfeld 1985; Yong and Seinfeld 1992; Jacobson 1997ac; Lurmann et al. 1997; Whitby and McMurry 1997; Wilck and Stratmann 1997; Fitzgerald et al. 1998; Harrington and Kreidenweis 1998; Pilinis et al. 2000).

Sectional methods

Sectional method is a kind of discrete aerosol size distribution approach, which was originally developed by Gelbard et al. (Gelbard and Seinfeld 1980; Gelbard et al. 1980) with a variety of subsequent improvements and adaptations (Gelbard 1990; Yong and Seinfeld 1992; Jacobson 1997b; 1997c; Trautmann and Wanner 1999). In a sectional representation, the particle size range is divided into a finite number of sections and all particles within a given size section are represented with the same composition. While computational and measurement capabilities place constraints on the maximum number of sections, in principle the size resolution of a sectional representation is limited only by the number of sections used. Most importantly, by classifying particles into distinct size bins, it allows particles of different sizes to have different compositions.

In the original sectional method (Gelbard and Seinfeld 1980; Gelbard et al. 1980), the sectional size boundaries are fixed and particles in the same section are averaged to have a uniform composition. The middle of a size bin is usually used to represent the size of all particles. The fixed sectional method has a very simple size structure, and it can cover a wide range of particle sizes if the sectional boundaries are set big enough. It is especially convenient for three-dimensional air quality models; the particles from different emission sources and grid cells are classified using the same size boundaries and can be easily assigned to the correct size bin, which is essential for air quality models normally containing 10^3 - 10^6 grid cells (Jacobson 1997c).

The most prominent disadvantage of the fixed sectional method is the numerical diffusion that occurs when simulating condensational growth. When one particle grows to a larger size bin because of condensation, its size is set as exactly the same as all the other particles in that bin, though its size may be only slightly larger than the lower section boundary. This artificial size adjustment occurs for each time step and for all particles that transfer from one size bin to another, leading to a numerical diffusion of the size distribution.

In order to address this shortcoming, the moving sectional (Gelbard 1990) and moving center sectional (Jacobson 1997b, a) methods have been developed. In the moving sectional method, the boundaries of sections are no longer fixed. With the growth of particles, instead of moving particles from one section to another, the section itself moves. This method does eliminate the numerical diffusion associated with condensational growth, but combining distributions with different size boundaries becomes extremely difficult and produces its own errors. This limits its usage in air quality models, where distributions are transported among thousands of grid cells.

In the moving center sectional method, the boundaries of sections are still fixed, but the diameter of particles is not limited to the middle of size range, varying within the size bin. Since it has similar accuracy as the moving sectional method in representing aerosol distribution associated with aerosol growth and as the fixed sectional method in combining distributions from different grid cells (Jacobson 1997a; Zhang et al. 2000), this method has been widely used in many newly released air quality models (Pilinis et al. 2000; Jacobson 2001a; Zhang et al. 2004). However, recent investigations suggest that severe numerical errors may be produced for condensation process by moving center sectional method. Because all the particles in a section move across the section boundary if the growth of particles is large enough, while no smaller size particles can grow to fill that section, artificial peaks and valleys in the distribution may be produced (Sun et al. 2004).

Modal methods

Modal methods were first introduced by Whitby (1978) and have continued to be refined (Binkowski and Shankar 1995; Whitby and McMurry 1997; Whitby et al. 2002). A modal representation treats the aerosol size distribution as a set of individual, typically lognormal, distributions or modes. In a lognormal modal distribution (Seigneur et al. 1986; Seinfeld and Pandis 1998), the aerosol distribution is defined by the parameters of lognormal equations. A modal representation of the aerosol size distribution assumes components in each mode are well mixed such that all particles within a given mode have the same composition. Different modes, however, may have different compositions.

Consequently, particles of the same size may belong to different modes and have different compositions.

As shown in Figure 2.1, ambient aerosol size distributions generally have 2 or 3 well-defined peaks. So, in the application of modal method in air quality model simulations, 2 or 3 modes are typically used. Each modal distribution is defined by three parameters: median diameter, standard deviation, and total number (or mass, volume, surface area, etc. depending on the particle characteristics of interest), such that 9 parameters can define an entire size distribution if represented by 3 modes. Compared with sectional methods, modal method has much faster simulation speed and less computational requirements, but the accuracy of modal method is determined by how well the assumed analytical function fits the real size distribution profile (Zhang et al. 2000; Zhang et al. 2002).

Several inherent shortcomings limit the application of modal methods. First, a modal distribution is not well-suited for aerosol coagulation process. When two particles from different modes coagulate, the position of coagulated particle can only be determined by assumption or other specific requirements (Binkowski and Shankar 1995). The difficultly of combining newly emitted aerosol distribution with existing distribution is another disadvantage of modal method. With the continuous emission of new particles and the growth of older ones, particles of different sizes or from different modes will need to be combined in a single mode, producing diffusional errors. Finally, the modal method is not suitable for representing in detail a multicomponent system with highly diverse properties. If particle populations with different composition are treated separately, the number of modes required will increase dramatically and the model will not be simple anymore. So, modal distribution is usually used in large scale applications where computational efficiency is more important than a detailed treatment of aerosol chemical composition and size distribution.

Conversion methods

An issue in working with sectional and modal aerosol distributions is the challenge of converting one size distribution representation to another. One of the difficulties in aerosol modeling is adequately describing the compositional heterogeneity of an aerosol population. Sectional methods are able to represent differences in composition as a function of particle size, while modal methods can represent compositional differences among particles of the same size. Hybrid modal-sectional models, where aerosol size distribution is represented by sectional method for some simulation processes and modal method for others, are one alternative to overcome the shortcomings of sectional and modal methods, but require conversion between sections and modes. In the UAM-VPM air quality model (Douglas 2002) this type of hybrid scheme has been introduced by adding modal discretization and sectional remodalization into aerosol processes.

Since modal and sectional methods each take a different approach to representing the aerosol distribution, each contains unique size and compositional information, which may be lost when converting from one form to the other. An effective conversion method is needed which is both accurate and computationally efficient. It should be able to convert multicomponent aerosol size distributions between sectional and modal forms, while preserving total aerosol and individual component mass and their distributions. In model UAM-VPM, a highly simplified hybrid system is used, where there are only 2 sections (0.1 - 2.5μm and 2.5 - 10μm) in sectional distribution, and 2 modes (with fixed standard deviation and median diameter) in modal distribution. Conversion between sectional and modal distributions is quite simple in this case, because each section correlates directly with one mode. During conversion from sectional to modal distribution, all the mass in section 1 goes to mode 1 and the mass in section 2 goes to mode 2. Aerosol mass will go back to the same sections when converting modal to sectional distribution. Many aerosol models use much higher resolution, however, with 8 or more sections in a sectional distribution and 3 or more modes without fixed median diameters or standard deviations in a modal distribution. Accurately converting a multicomponent aerosol distribution from multiple sections to modes with variable standard deviation and median diameter is still a challenge.

Representation of aerosol mixing states

Aerosol particles are typically assumed to exist as either an internal or external mixture. Under an internal mixture definition, all particles in the same size bin or mode have exactly the same chemical composition, and behave exactly the same when interacting with the surrounding gas phase. This definition makes the modeling of multicomponent aerosols much easier, because only one size distribution is needed and it is independent of the particles emission sources and composition (Russell and Seinfeld 1998). Actually, ambient aerosol particles come from different sources, so different components may exist in particles of the same size (Hildemann et al. 1991; Rogge et al. 1993; Noble and Prather 1996; FassiFihri et al. 1997; Gard et al. 1998; Naoe and Okada 2001). It is more realistic to define aerosol particles as an external mixture, where particles of a given size may have different chemical compositions. When these particles interact with gas phase or other particles, each particle will maintain a separate evolutionary history (Jacobson 2001b).

Until recently, internally mixed particles have been used in most air quality models, mainly because of limitations in computational power and our understanding of aerosol properties (Wexler et al. 1994; Binkowski and Shankar 1995; Jacobson 1997b, a; Meng et al. 1998; Sun and Wexler 1998b, a; Binkowski and Roselle 2003; Zhang et al. 2004). Whether represented by a modal or sectional method, there is only one aerosol size distribution in these models, and the compositional differences between particles of the same size, but from various sources, is neglected. Since an internal mixture is only an approximation of the real aerosol mixing state, some simulation error is inevitable. Because an external mixture is often much closer to the actual aerosol mixing state, the use of externally mixed particle distributions in air quality models can decrease the errors resulting from assuming an internal mixture. Recent progress on the research of externally mixed particles makes this implementation realistic (Kleeman et al. 1997; Russell and Seinfeld 1998; Kleeman et al. 1999; Bhave et al. 2002; Jacobson 2002; Mysliwiec and Kleeman 2002; Held et al. 2004).

In an external mixture model developed by Jacobson (Jacobson 1997c; Jacobson 2002), there are a total of 42 particle phase components. Initially, there are only 4 aerosol distributions from emission sources, which are treated as externally mixed particles. If a particle is formed from coagulation of two different types of particles, or grows as other components form a coating on black carbon, it is assigned to a binary distribution and treated as partly internal mixture. All the particles resulting from a combination of three or more externally mixed distributions are treated as a single internal mixture. In all, there are 18 possible distributions existing. Simulation results show that, under the conditions tested, coagulation is the main process that mixes different types of aerosol particles, and that the degree of externally mixed particles is decreased by coagulation and condensation processes.

Kleeman has developed a source-oriented Lagrangian air quality model (Kleeman et al. 1997; Kleeman et al. 1999; Kleeman and Cass 2001; Bhave et al. 2002) that is different from the box model used by Jacobson. In this model the emitted particles in an urban area are differentiated to several sources, such as gasoline engines, diesel engines, paved road dust, and so on. Each source distribution has its own size and component distribution, and evolves separately in the atmosphere. Both organic and inorganic components are tracked in gas and particle phase. Coagulation and nucleation processes are not considered in the model. The model was run using both externally mixed and internally mixed representations to simulate conditions during the 1987 Southern California Air Quality Study (SCAQS). The simulation results showed that only the external mixture model can predict chemical composition differences between particles of the same general size, and successfully reproduce the bimodal feature of the observed aerosol size distribution.

The distinction between internally and externally mixed particles is not precise in most situations. When two externally mixed particles with different composition coagulate together to form a new particle, this new particle could be defined as an internal mixture because it contains both components of the former two (Jacobson 2001b, 2002). For example, in a soot particle system, the freshly emitted particles from different combustion sources are external mixtures. But within minutes of emission, these soot particle size distributions have been shown to evolve substantially, mainly by coagulation process (Vignati et al. 1999; Naoe and Okada 2001; Jacobson and Seinfeld 2004). As the different types of soot particles mix with each other, compositional differences between particles are reduced, and all the particles could be grouped together as an internally mixed distribution. But compared with an aerosol distribution from sea spray, it is still an external mixture. Thus, the definition of external and internal mixtures is a relative concept. Within an aerosol model, calculation speed and accuracy requirements will play a major role in choosing the level of detail for representing compositional mixtures.

Secondary organic aerosol (SOA)

As a complex mixture, both inorganic and organic components have been found in aerosol particles. Organic compounds cover a very wide range of molecular forms, and this makes their complete characterization extremely difficult (Carter 1990; Jacobson et al. 2000; Griffin et al. 2002b). Some are emitted directly from emission sources as particles, and this is call primary organic aerosol. But many are formed by photochemical reactions in the gas phase and move to the particle phase through gas-to-particle conversion process. This kind organic particulate matter is named as secondary organic aerosol (SOA) (Pandis et al. 1992).

Secondary organic aerosol is formed in two steps. First, volatile organic compounds are oxidized in the gas phase resulting in new organics with lower vapor pressure. Then, these newly produced semivolatile organic compounds (SVOCs) can partition to the aerosol phase via condensation or nucleation. Currently, hundreds of

SVOCs and oxidation reactions have been found, but most are still unknown. Mapping all of the exact chemical pathways leading to the formation of SOA is nearly impossible and is unrealistic for aerosol models. Instead, a simplified model is usually used in representing the formation of SOA components by the reaction of a hydrocarbon (HC) precursor with OH radical:

$$HC + OH \rightarrow \alpha_1 S_1 + \alpha_2 S_2 + \ldots + \alpha_n S_n \tag{2.1}$$

where α_i is the mass stoichiometric coefficient of semivolatile organic S_i. Besides OH radical, organic precursors also can be oxidized by O_3 or NO_3 (Pandis et al. 1992).

The partitioning of SOA occurs via an absorption mechanism, where SVOCs in the gas phase partition into an existing liquid aerosol phase consist of absorbing materials (Pankow 1994; Odum et al. 1996). The partitioning of SVOC i can be described by partitioning coefficient K_i:

$$K_i = \frac{F_i}{A_i * M_o} \tag{2.2}$$

where K_i is a temperature-dependent equilibrium partitioning constant; F_i and A_i are the mass concentrations of semivolatile species i in the particle and gas phases, respectively; and M_o is the concentration of absorbing aerosol.

Based on the absorption process, the partitioning coefficient can be expressed as:

$$K_i = \frac{RT}{MW \xi_i p_i^o} \tag{2.3}$$

which is a function of physical and thermodynamic properties of the semivolatile compounds. R is the gas constant, T is temperature, MW is the mean molecular weight of the absorbing aerosol phase, ζ_i is the activity coefficient of compound i in aerosol phase, and p_i^0 is the vapor pressure of compound i as a liquid.

The mass flux of a semivolatile compound *i* to a single aerosol particle can be written as (Wexler and Seinfeld 1990; Meng and Seinfeld 1996):

$$J_i = 2\pi D_p D_i \frac{C_{\infty,i} - C_{s,i}}{\frac{2\lambda}{\alpha_i D_p} + 1} \quad (2.4)$$

where D_p is particle diameter, D_i is the diffusivity of species *i*, $C_{\infty,i}$ is the concentration of *i* in the bulk gas phase, $C_{s,i}$ is the gas-phase concentration in equilibrium with the aerosol particle, λ is the mean free path of air, and α_i is the accommodation coefficient of species *i* on the particle.

There are two widely used approaches to modeling the partitioning of semivolatile species between gas and particle phases. One is thermodynamic equilibrium method, and another is fully dynamic mass transfer method (Meng and Seinfeld 1996; Bowman et al. 1997; Jacobson 1997a; Meng et al. 1998; Capaldo et al. 2000; Zhang et al. 2000; Moya et al. 2002). In thermodynamic equilibrium method, where particles across all sizes are treated as a bulk aerosol phase, it is assumed that gas and aerosol phases are always in equilibrium. In the fully dynamic mass transfer method, where particles in each section are treated separately, equation (2.4) is solved to determine mass transfer between gas and aerosol in each section. A hybrid partitioning approach based on these two methods has recently been provided, where the equilibrium of small particles (D_p<1 μm) with gas phase is based on thermodynamic equilibrium, while the partitioning between large particles and gas phase is calculated by fully dynamic mass transfer method (Jacobson 1997a; Capaldo et al. 2000).

CHAPTER III

CONVERSION OF MULTICOMPONENT AEROSOL SIZE DISTRIBUTIONS FROM SECTIONAL TO MODAL REPRESENTATIONS

Published as:

Lu, J. and Bowman, F.M., “Conversion of multicomponent aerosol size distributions from sectional to modal representations”, *Aerosol Science & Technology*, 38(4): 391-399, 2004

Abstract

A new method for converting a multicomponent aerosol size distribution from sectional to modal form is presented. The sectional distribution is fit with multiple lognormal modes using a non-linear least square regression that considers both the overall mass distribution and individual component distributions. The new method is compared to other conversion methods that assign sections to modes arbitrarily or that fit only the total mass distribution. Results of conversion tests using example distributions show that the multicomponent fit method is able to define a modal distribution that more accurately represents the original sectional distribution than do other methods. Total and component mass are conserved, the size, shape, and location of peaks match the original distribution, and modal compositions allocate components to the same size range as in the sectional representation. It is also able to convert distributions with relatively few size sections or where the size sections do not span the entire distribution, and does not propagate errors when distributions are converted repeatedly between sections and modes.

Introduction

Aerosol dynamic processes (i.e., coagulation, nucleation, condensation, and deposition) that govern aerosol formation, growth and evolution depend on the number, size, and composition of particles. In the atmosphere, these aerosol characteristics determine the influence of particles on health, climate, cloud formation, and visibility (Seinfeld and Pandis 1998; Hinds 1999; Pope 2000). To accurately predict these impacts, the size and composition distribution of the aerosol must be known. The true aerosol distribution encompasses a population of individual particles, each with its own distinct mass, shape and composition. Since in most cases an exact accounting for each individual particle is impossible, alternate representations of the size distribution are required.

Two of the most common approaches for describing aerosol size distributions are sectional and modal methods. Both have been widely used in atmospheric models (Warren and Seinfeld 1985; Yong and Seinfeld 1992; Jacobson 1997a; Jacobson 1997c; Lurmann et al. 1997; Whitby and McMurry 1997; Wilck and Stratmann 1997; Fitzgerald et al. 1998; Harrington and Kreidenweis 1998). Sectional methods were originally developed by Gelbard and Seinfeld (1980a; 1980b) with a variety of subsequent improvements and adaptations (Gelbard 1990; Yong and Seinfeld 1992; Jacobson 1997b, a; Trautmann and Wanner 1999). In a sectional representation the particle size range is divided into a finite number of sections and all particles within a given size section are represented with the same composition. Modal methods were first introduced by Whitby (1978) and have continued to be refined (e.g., Binkowski and Shankar 1995; Whitby and McMurry 1997; Whitby et al. 2002). A modal representation treats the aerosol size distribution as a set of individual, typically lognormal, distributions or modes. All particles within a given mode are represented with the same composition.

One of the difficulties in aerosol modeling is adequately describing the compositional heterogeneity of an aerosol population. Sectional methods are able to represent differences in composition as a function of particle size. Modal methods can represent compositional differences among particles of the same size. Since modal and sectional methods each take a different approach to representing the aerosol distribution, each contains unique size and compositional information, which may be lost when converting from one form to the other.

Methods for accurately converting sectional distributions to modal form have several potential applications. To be used within modal air quality models, size-segregated field measurements must be converted from sections to modes. Hybrid sectional-modal models, such as UAM-VPM (Douglas 2002), where certain aerosol processes use a sectional representation, and others use a modal representation, also require conversion between sections and modes. A reliable conversion technique would also provide an additional approach for directly comparing sectional and modal distributions.

We present here a new method for converting a multicomponent aerosol size distribution from sectional to modal form. In this method, the overall sectional size distribution is fit with multiple lognormal modes. Additionally, components within a section are distributed between modes such that all particles corresponding to a given mode have similar compositions. The method is evaluated with example size distributions and the results are compared to those from other conversion methods.

Size Distribution Representations

In a sectional size distribution, the exact distribution of aerosol particles is approximated by a discrete number of sections. The mass size distribution of a multicomponent aerosol with *NC* individual components can be written in a sectional representation with *NS* sections as (Warren and Seinfeld 1985)

$$M_{ij} = \int_{d_{p\,j-1}}^{d_{p\,j}} q_i(d_p)\,dd_p \tag{3.1}$$

where M_{ij} is the mass of component i in size section j, $q_i(d_p)$ is the mass size distribution function of component i, and $d_{pj\text{-}1}$ and d_{pj} are, respectively, the smallest and largest particle diameters in section j. The sectional distribution is thus defined by the variables M_{ij} and d_{pj}.

In a modal distribution, the aerosol distribution is represented as the sum of several individual distributions or modes (Whitby and McMurry 1997)

$$q(d_p) = \sum_{k=1}^{NM} q_k(d_p) \tag{3.2}$$

where $q(d_p)$ is the approximated total mass size distribution, $q_k(d_p)$ is the mass size distribution of mode k, and NM is the total number of individual modes. Modes are often described with a lognormal equation (Seigneur et al. 1986; Seinfeld and Pandis 1998)

$$q_k(d_p) = \frac{Q_k}{(2\pi)^{1/2}\log(\sigma_k)} \times \exp\left(-\frac{1}{2}\left(\frac{\log(d_p) - \log(d_{pk})}{\log(\sigma_k)} \right)^2 \right) \tag{3.3}$$

where Q_k is the total mass in mode k, and σ_k and d_{pk} are the standard deviation and median diameter of mode k. For multicomponent aerosols the mass of component i in mode k, Q_{ik}, can be defined as

$$Q_{ik} = Q_k x_{ik} \tag{3.4}$$

where x_{ik} is the mass fraction of component *i* in mode *k*. The variables, Q_k, σ_k, d_{pk}, and x_{ik}, therefore, define a lognormal modal distribution.

Conversion Method

In this part of research we are interested in converting a multicomponent aerosol from one size distribution representation to the other. Recall that a sectional distribution is defined by the parameters M_{ij} and d_{pj}, and a modal distribution is defined by Q_k, σ_k, d_{pk}, and x_{ik}. It is important to note a key difference in how sectional and modal distributions are constructed. A modal distribution spans the entire size range, but a sectional distribution includes only the size range of its sections. For an aerosol distribution that extends beyond the upper or lower section boundaries, a portion of the particle mass will not be included in a sectional distribution, while it will be accounted for in a modal distribution. As a result the total mass in a sectional representation may be less than that in a modal representation of the same distribution.

$$\sum_i \sum_j M_{ij} \le \sum_i \sum_k Q_{ik} \tag{3.5}$$

The left-hand term in equation (3.5) is the sum of all components in all sections and the right-hand term is the sum of all components in all modes. To compare sectional and modal quantities directly we can define a modified modal component mass, Q_{ik}', which is the mass of component *i* from mode *k* that lies within the size boundaries, d_{p0} and d_{pNS}, of a given sectional distribution.

$$Q_{ik}' = \int_{d_{p0}}^{d_{pNS}} q_k(d_p) x_{ik} \, dd_p \tag{3.6}$$

Whereas Q_{ik} is the integrated mass over all sizes, Q_{ik}' includes only the mass within the size range defined by the sectional distribution. When the sectional size range is large enough to capture the entire distribution, Q_{ik} and Q_{ik}' will be essentially the same.

The goal, therefore, in converting between sections and modes is to calculate the parameters for one type of distribution given the parameters of the other type. We present first the relatively straightforward process of converting a modal to a sectional distribution, and then consider in detail the more difficult sectional to modal conversion.

Modal to Sectional Conversion

When converting a modal distribution (Q_k, σ_k, d_{pk}, and x_{ik}) to a sectional distribution (M_{ij}, d_{pj}), the section size boundaries, d_{pj}, must first be specified. Then the multicomponent modal distributions are mapped into the size sections to determine the mass of each component in each section, M_{ij}.

$$M_{ij} = \sum_{k=1}^{NM} \left(\int_{d_{p\,j-1}}^{d_{p\,j}} \frac{Q_k x_{ik}}{(2\pi)^{1/2} \log(\sigma_k)} \times \exp\left(-\frac{1}{2} \left(\frac{\log(d_p) - \log(d_{pk})}{\log(\sigma_k)} \right)^2 \right) dd_p \right) \tag{3.7}$$

The integral term in equation (3.7) represents the mass of component i from mode k that will be placed in section j, which we will define as T_{ijk}.

$$T_{ijk} = \int_{d_{p\,j-1}}^{d_{p\,j}} q_k(d_p) x_{ik} dd_p \tag{3.8}$$

The variable T_{ijk} combines both sectional and modal information. Using T_{ijk} as the basis for what we consider the true aerosol distribution, a correct sectional distribution will have sectional masses, M_{ij}, that are a subset of T_{ijk}.

$$M_{ij} = \sum_{k=1}^{NM} T_{ijk} \tag{3.9}$$

Similarly, a correct modal distribution requires that Q_{ik}' values comprise a different subset.

$$Q_{ik}^{'} = \sum_{j=1}^{NS} T_{ijk} \tag{3.10}$$

Converting modes to sections using equation (3.7) is a two-step procedure wherein Q_{ik} is first converted to T_{ijk} by integrating over sections j, followed by the summation over modes to reduce T_{ijk} to M_{ij}. Unfortunately, a similarly simple procedure is unavailable for the reverse process of converting sections to modes.

Sectional to Modal Conversion

Unlike modal to sectional conversion, where the continuous modal functions are integrated to precisely determine the mass in discrete sections, the reverse process of converting sections to modes is not exact. The challenges in doing this can be illustrated with the following example. A sectional distribution with 8 sections and equal amounts of A and B is shown in Figure 3.1. Component A is concentrated in the smaller size sections, and component B is found primarily in the larger sections. In converting this, or any, distribution from a sectional to a modal representation, there are at least three criteria for what we may consider a proper fit.

First, to be physically meaningful, mass must be conserved. Both the total aerosol mass and the mass of individual components must be the same in modal and sectional representations. Second, the overall modal size distribution should be a good fit to the sectional distribution. As seen with the mode curves in Figure 3.1, the number of modes and their height, width, and position should be such that the shape of the modal distribution is as close as possible to that of the sectional distribution.

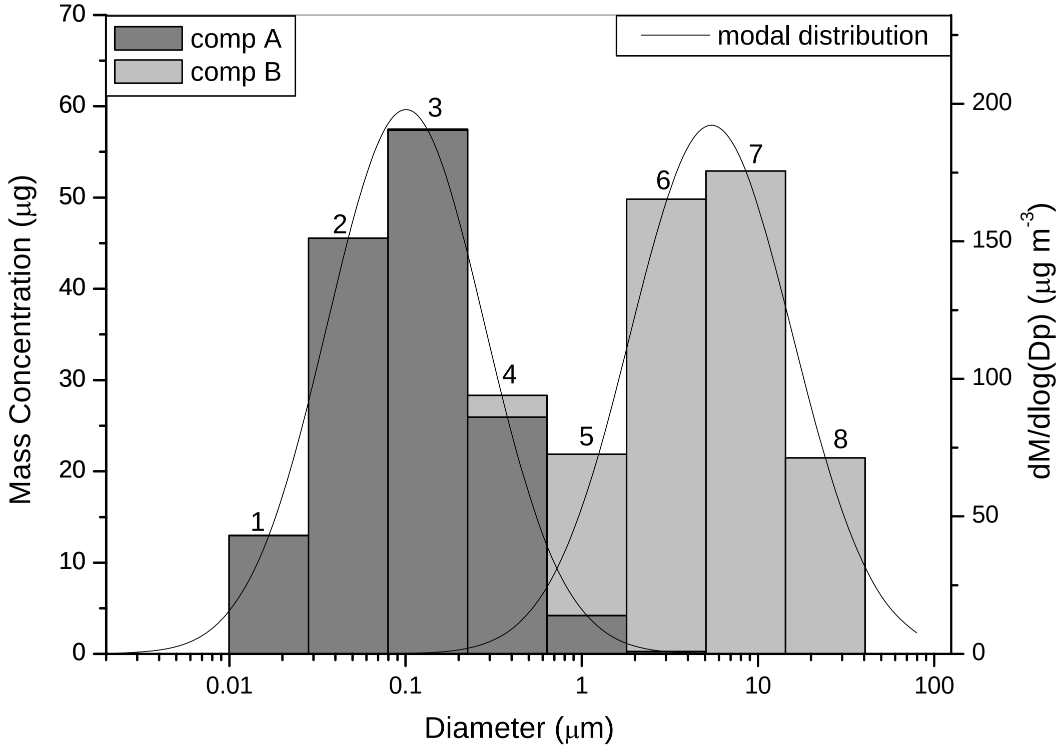

Figure 3.1 Sample aerosol distribution with two overlapping populations.

Third, for a multicomponent distribution, components should be allocated to the correct mode. The goal is to create compositionally distinct modes, which if converted back to sections would result in a similar composition distribution. In Figure 3.1, for example, there appear to be two distinct types of particles, one that is pure A and another that is pure B. In this case, component A should be assigned exclusively to the smaller mode, and component B to the larger mode. Difficulties arise when considering sections where modes overlap. A sectional representation assumes particles have the same composition, which has the effect of mixing particles of different compositions. When converted to modes, sections need to be unmixed so that particles of similar composition are placed in the same mode. In Figure 3.1, the middle sections contain significant amounts of both A and B. They should be unmixed, so that particles assigned to the smaller mode are made of pure A, instead of a mixture of A and B. The best way to unmix sections while meeting the first two criteria is not obvious and will be explored in the following sections.

There are various possible approaches for converting sections to modes. We will consider three different methods: (1) an *arbitrary fit*, where each section is assigned to a specific mode; (2) a *total mass fit*, where modes are fit to sections based on total aerosol mass without unmixing sections; and (3) a *multicomponent fit* that attempts to meet all three criteria for a proper fit by fitting modes based on total aerosol mass and component mass fractions.

Arbitrary Fit

Perhaps the simplest approach for fitting modes to sections is to assign sections in a given size range to a specific mode. For this work, section boundaries at 0.078 µm and 2.5 µm are used as the dividing line between nuclei, accumulation and coarse modes. All sections larger than 2.5 µm are assigned to the coarse mode, those between 2.5 µm and 0.078 µm are assigned to the accumulation mode, and those sections less than 0.078 µm are assigned to the nuclei mode. The median diameters of the three modes, d_{p1}, d_{p2}, d_{p3}, are set as 0.03, 0.3 and 6 µm, and the standard deviations, $\sigma_1, \sigma_2, \sigma_3$, are 1.7, 2.0 and 2.2, respectively, based on values suggested for atmospheric aerosol emissions (Binkowski 1999).

The arbitrary fit method is used in some form to prepare emissions data for most modal air quality models (Binkowski and Shankar 1995; Ackermann et al. 1998; Binkowski and Roselle 2003; Mebust et al. 2003). Particulate emissions inventories typically report $PM_{2.5}$ and PM_{10} mass emissions, in what is essentially a 2-section distribution. Because no additional size distribution information is available, $PM_{2.5}$ emissions are assigned to the accumulation mode, and particles larger than 2.5 µm are placed in the coarse mode. Modes created by this method may or may not be a good fit to the original sectional distribution, since most of the modal parameters are arbitrarily specified. Referring back to the three criteria for a proper fit, only the first criterion, conservation of mass, is met in all cases.

Total mass fit

To create modes that are a better fit to sections, a numerical curve fitting routine can be used to minimize the difference between modal and sectional distributions. In the total mass fit method, the modal parameters which describe the total mass distribution, Q_k, σ_k, d_{pk}, are determined using a non-linear least square regression (More et al. 1980). Equations (3.11) to (3.14) in Table 3.1 comprise the set of equations to be minimized by regression for the total mass fit.

Equation (3.11) fits total mass in individual sections, where the first term is mass within a section as defined by the sectional distribution, and the second term is total mass within that size range from all modes in the modal distribution. The T_{jk} term is an integral over the size range of section j

$$T_{jk} = \int_{d_{p(j-1)}}^{d_{pj}} q_k(d_p)dd_p \tag{3.19}$$

and is the mass from mode k that lies within the size boundaries of section j. By minimizing the error in equation (3.11) for each section, a modal distribution is produced that resembles the sectional distribution from which it was derived. Equation (3.12) specifies conservation of total mass, where the first term is total aerosol mass in all sections, and the second is total aerosol mass in all modes that fall within the sectional size range. Equations (3.13) and (3.14) specify non-negative values for Q_k and σ_k. To account for the different magnitudes of terms in these equations, equations (3.11) to (3.13) are normalized by total mass, $\Sigma_i\Sigma_jM_{ij}$, so that terms in all four equations are approximately of order 1. Additionally, to ensure non-negative values, equations (3.13) and (3.14) are further weighted by a factor of 10.

Table 3.1 Regression equations for total mass fit and multicomponent fit conversion methods.

Equation Number	Equation	Normalization factor	Weighting factor
Regression equations for total mass fit.			
(3.11)	$\sum_{i=1}^{NC} M_{ij} - \sum_{k=1}^{NM} T_{jk} = 0$	$\Sigma_i \Sigma_j M_{ij}$	1
(3.12)	$\sum_{j=1}^{NS} \sum_{i=1}^{NC} M_{ij} - \sum_{j=1}^{NS} \sum_{k=1}^{NM} T_{jk} = 0$	$\Sigma_i \Sigma_j M_{ij}$	1
(3.13)	$Q_k - \lvert Q_k \rvert = 0$	$\Sigma_i \Sigma_j M_{ij}$	10
(3.14)	$\sigma_k - \lvert \sigma_k \rvert = 0$	1	10
Additional regression equations for multicomponent fit.			
(3.15)	$M_{ij} - \sum_{k=1}^{NM} T_{jk} x_{ik} = 0$	$\Sigma_j M_{ij}$	1
(3.16)	$\sum_{j=1}^{NS} M_{ij} - \sum_{j=1}^{NS} \sum_{k=1}^{NM} T_{jk} x_{ik} = 0$	$\Sigma_j M_{ij}$	1
(3.17)	$x_{ik} - \lvert x_{ik} \rvert = 0$	1	10
(3.18)	$\sum_{i=1}^{NC} x_{ik} - 1 = 0$	1	1

A modal distribution with *NM* modes will have *3*NM* unknown parameters. Regression equations (3.11) and (3.12) provide *NS+1* equations for a sectional distribution containing *NS* sections. As a result, the total mass fit method requires at least *3*NM-1* sections to fit a modal distribution with *NM* modes. To create a distribution with 2 modes, for example, a sectional distribution with at least 5 sections is needed, and 3 modes require 8 or more sections. If the number of sections is less than the minimum required, standard deviations, and/or median diameters of the modes can be specified as in the arbitrary fit.

Composition is not considered in the total mass fit regression, but is accounted for in a second step that calculates modal composition, x_{ik}, as an average of the sectional mass fractions, x_{ij}, weighted by the mass in a section going to that mode, T_{jk}

$$x_{ik} = \frac{\sum_{j=1}^{NS} T_{jk} x_{ij}}{\sum_{j=1}^{NS} T_{jk}} \tag{3.20}$$

Equation (3.20) has the effect of dividing the mass in a section between each of the *NM* modes, while assuming the mass sent to each mode has the same composition as that of the entire section. The total mass fit makes no attempt to unmix components in a section when allocating them to modes.

This step of allocating components to modes introduces some error, especially for modes with large areas of overlap. In Figure 3.1, for example, section 5 contains both A and B. The total mass fit method will divide this section between the two modes and both portions will have the same composition of A and B, causing some A to be assigned to the larger mode and some B to the smaller mode. As a result, while the total mass fit method produces a modal distribution that meets the mass conservation and overall mass fit criteria, it may not correctly distribute components among modes.

Multicomponent fit

The new multicomponent fit method we have developed considers component mass and mass fractions in addition to total mass when performing the non-linear least square regression. By fitting to total mass and composition simultaneously, it is able to unmix the section compositions and create a modal distribution that correctly mirrors the original sectional distribution. Unlike the arbitrary and total mass approaches, the multicomponent fit can satisfy all three criteria for a successful conversion from sections to modes.

The multicomponent fit regression includes equations (3.11) to (3.14) from the total mass fit method plus composition equations (3.15) to (3.18) as shown in Table 3.1. Using known values of sectional parameters M_{ij} and d_{pj}, the non-linear least squares routine determines values of modal parameters Q_k, σ_k, d_{pk}, and x_{ik} that minimize the error in these equations.

The primary additional equation included in the regression is equation (3.15), which fits the modal component distribution to the sectional component masses. The first term is the mass of component i in section j from the sectional distribution and the second term is the same quantity derived from the modal distribution. Equation (3.16) specifies conservation of mass for each component, where the first term is total mass of component i in the sectional distribution and the second term is total mass of component i in the modal distribution. Equations (3.17) and (3.18) require that modal mass fractions be non-negative and sum to 1.

As with the total mass fit, equations (3.11) to (3.13) are normalized by total mass, $\Sigma_i \Sigma_j M_{ij}$. The new component mass equations, (3.15) and (3.16), are normalized by total component mass, $\Sigma_j M_{ij}$. Equations (3.13), (3.14) and (3.17) are also weighted by a factor of 10 to provide a reasonable balance between the regression constraints when finding a solution. This set of weighting values was found to work well for several distributions examined in this study, but has not been widely tested on other distributions.

For a modal distribution with NM modes and NC components, there will be $3*NM+NC*NM$ unknown parameters. Equations (3.11), (3.12), (3.15), (3.16) and (3.18) provide $NS+NC+NC*NS+2$ equations. In general, as long as there are more sections than modes ($NM<NS$), the regression can find a realistic solution. As a result, for the same number of modes and components a multicomponent fit requires fewer sections than does a total mass fit.

The multicomponent fit method satisfies all three fitting criteria for converting sections to modes. Total and component masses are conserved, and both component and total mass distributions are fit to the original sectional distribution. An important feature is that particles of similar composition are gathered into the same mode, essentially unmixing populations that have been combined in a sectional distribution.

Method Evaluation

Figure 3.2 shows one of several hypothetical sectional distributions used to test our conversion method. This distribution has 12 sections, logarithmically spaced between 0.01 μm and 40 μm, and 3 components, A, B, and C. Component A is concentrated in the smaller sections, while components B and C are present in the larger sections with varying ratios. The individual component masses, M_{ij}, and section boundaries, d_{pj}, for this distribution are listed in Table 3.2.

Since there are not well-defined peaks in this sectional distribution, the overall size distribution could be represented reasonably well with three, two, or even one mode. The compositional distribution, however, suggests that there are at least two distinct populations of particles, a smaller diameter mode containing primarily component A and a larger diameter mode composed of mainly B and C. In the results presented here, a modal distribution with 3 modes was assumed when fitting the sectional distribution.

Table 3.2 Parameters for sectional distribution shown in Figure 3.2.

Section	Aerosol Diameter Range (μm)	Component Mass in Section (μg m^{-3})		
		A	*B*	*C*
1	0.010 – 0.020	0.035	0.000	0.000
2	0.020 – 0.039	3.575	0.000	0.000
3	0.039 – 0.078	9.528	0.000	0.000
4	0.078 – 0.156	9.940	0.000	0.000
5	0.156 – 0.312	14.173	0.000	0.000
6	0.312 – 0.625	20.109	0.000	0.000
7	0.625 – 1.25	20.391	0.286	0.123
8	1.25 – 2.5	9.407	6.781	2.906
9	2.5 – 5	2.522	13.431	5.756
10	5 – 10	0.009	13.024	8.682
11	10 – 20	0.000	3.059	3.059
12	20 – 40	0.000	0.139	0.324

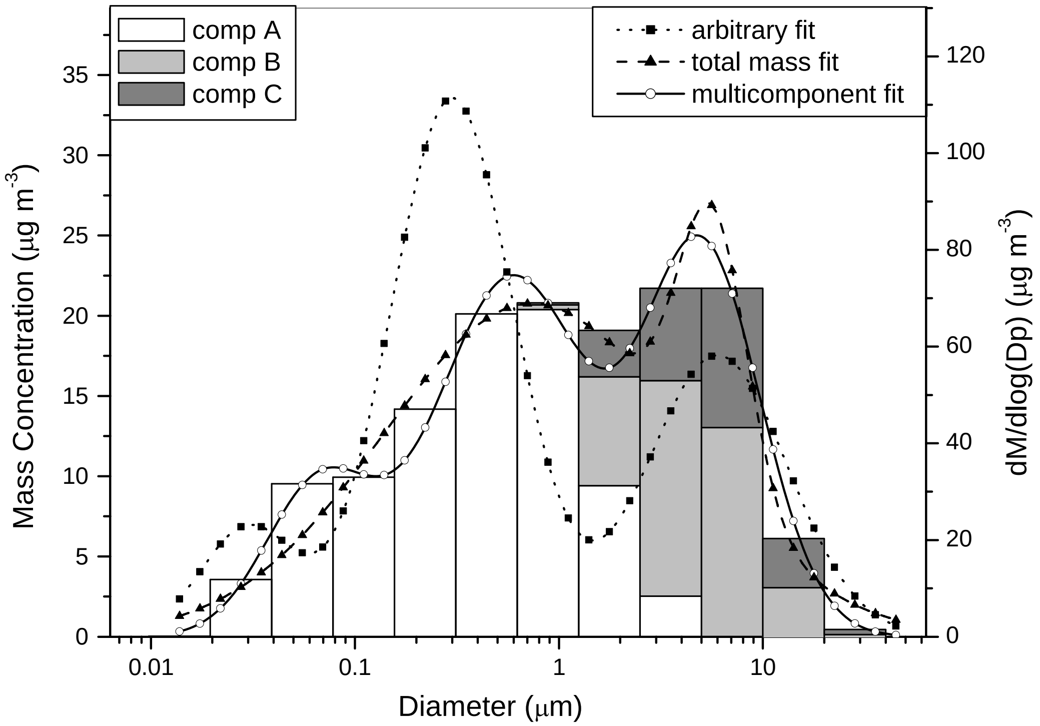

Figure 3.2 Original sectional distribution and converted modal distributions created using arbitrary fit, total mass fit, and multicomponent fit methods.

This sectional distribution was not derived from an exact lognormal distribution, and therefore does not have a modal distribution that fits it exactly. The three fitting criteria will be used to assess whether a calculated modal distribution provides a good fit to the sectional distribution. Another way to help judge the fitted modal distribution is to convert it back to sections, using equation (3.1). For the recreated sectional distribution, the overall size distribution and the distribution of components in sections should be similar to that in the original sectional distribution.

The sectional distribution, shown in Figure 3.2 and with parameters listed in Table 3.2, was converted to a modal distribution using the arbitrary, total mass, and multicomponent fit methods. Values of the modal parameters Q_k, d_{pk}, σ_k, and x_{ik} calculated by each of the three conversion methods are listed in Table 3.3. In Figure 3.2, conversion results for the arbitrary fit (marked with squares), total mass fit (triangles), and multicomponent fit (circles) are compared to the original sectional distribution. Figure 3.3 compares the recreated sectional distributions.

In the arbitrary fit method, sections are pre-assigned to modes and standard deviations are fixed, so mode 2 is forced to have a large peak height in order to maintain the same total mass as the broader sectional distribution. At the same time, mass in the larger diameter mode 3 is underestimated. As a result, the overall modal size distribution from the arbitrary fit method differs greatly from the original sectional distribution. When determining modal composition, there is no component B or C in the original sections smaller than 0.078 µm, so mode 1 is pure component A. Mode 2 is mostly component A, but also contains sizeable fractions of B (8.4%) and C (3.6%). Mode 3 is a mixture of B and C with a smaller amount of A (5%). These components are distributed evenly throughout the individual modes, so that when the modes are converted back to sections (Figure 3.3b), B and C now appear in 0.01 μm particles when originally they were only significantly present above 1.25 μm.

For the total mass fit method, one of the defined modes has a median diameter very close to zero (10^{-8} μm) and can be disregarded, leaving a distribution with 2 modes. Compared with results of the arbitrary fit method, mode 2 has a larger total mass and a much larger standard deviation, while mode 3 has much less mass and is narrower. The overall modal distribution from these two modes, shown in Figure 3.2, fits the sectional distribution quite well, considering the arbitrary shape of the sections.

Table 3.3 Converted modal distribution parameters.

	Converted Distributions								
	Arbitrary			*Total Mass*			*Multicomponent*		
Mode	1	2	3	1	2	3	1	2	3
Q_k (μg m^{-3})	13.1	84.1	50.0	-	125	23.7	21.0	69.0	57.6
σ_k	1.70	2.00	2.20	-	5.34	1.47	1.84	2.34	1.94
d_{pk} (μm)	0.03	0.30	6.00	10^{-9}	0.74	5.68	0.07	0.59	5.04
x_A (%)	100.0	88.0	5.1	-	71.5	4.5	99.9	99.8	0.0
x_B (%)	0.0	8.4	59.3	-	18.4	59.9	0.0	0.2	63.8
x_C (%)	0.0	3.6	35.6	-	10.1	35.6	0.1	0.0	36.2

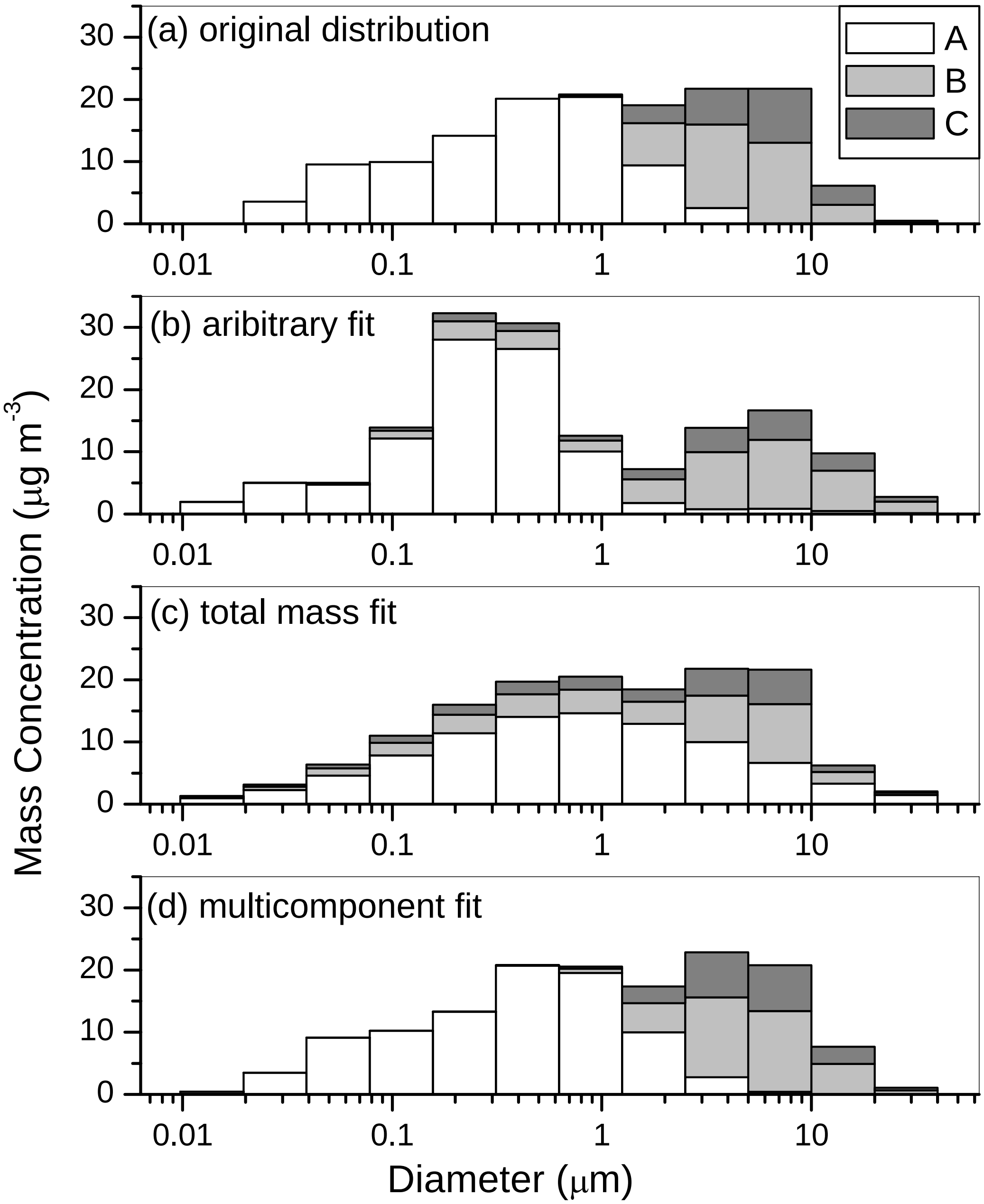

Figure 3.3 Original sectional distribution and sectional distributions created from converted modal distributions. (a) original sectional distribution; (b) arbitrary fit; (c) total mass fit; (d) multicomponent fit.

Since mode 2 contains most of the aerosol mass and more than the total mass of component A, components B and C make up almost 30% of mode 2. Mode 2 also has a large standard deviation that extends it over all sizes. Together, these factors have the effect of mixing most of the aerosol mass and spreading out the same composition of A, B and C over the entire size range, as seen in Figure 3.3c. The distribution of components is much different from the original one, showing even more diffusional error than the arbitrary fit method.

The multicomponent fit method produces modes that are different from those obtained with the total mass fit method because it fits the overall distribution and the component distributions at the same time. Modes 1 and 2 are composed almost exclusively of component A and together contain less mass than mode 2 from the total mass fit. Mode 3 is much larger than it was with the total mass fit and contains essentially all of components B and C. The multicomponent fit method is able to separate component A from components B and C into distinct modes by adjusting the modal parameters that define the overall mass size distribution. The total mass fit method, which ignores composition when fitting the size distribution, gives the best fit of the overall size distribution, but misrepresents the allocation of components. The size distribution from the multicomponent fit method is not quite as accurate, but the component distribution is much more consistent with the original sections.

Another advantage of the multicomponent fit method is that composition errors do not propagate when a distribution is converted repeatedly between sections and modes. To demonstrate this, the sectional distribution in Figure 3.2 was converted to modes and back to sections 5 times using each of the conversion methods. The resulting sectional

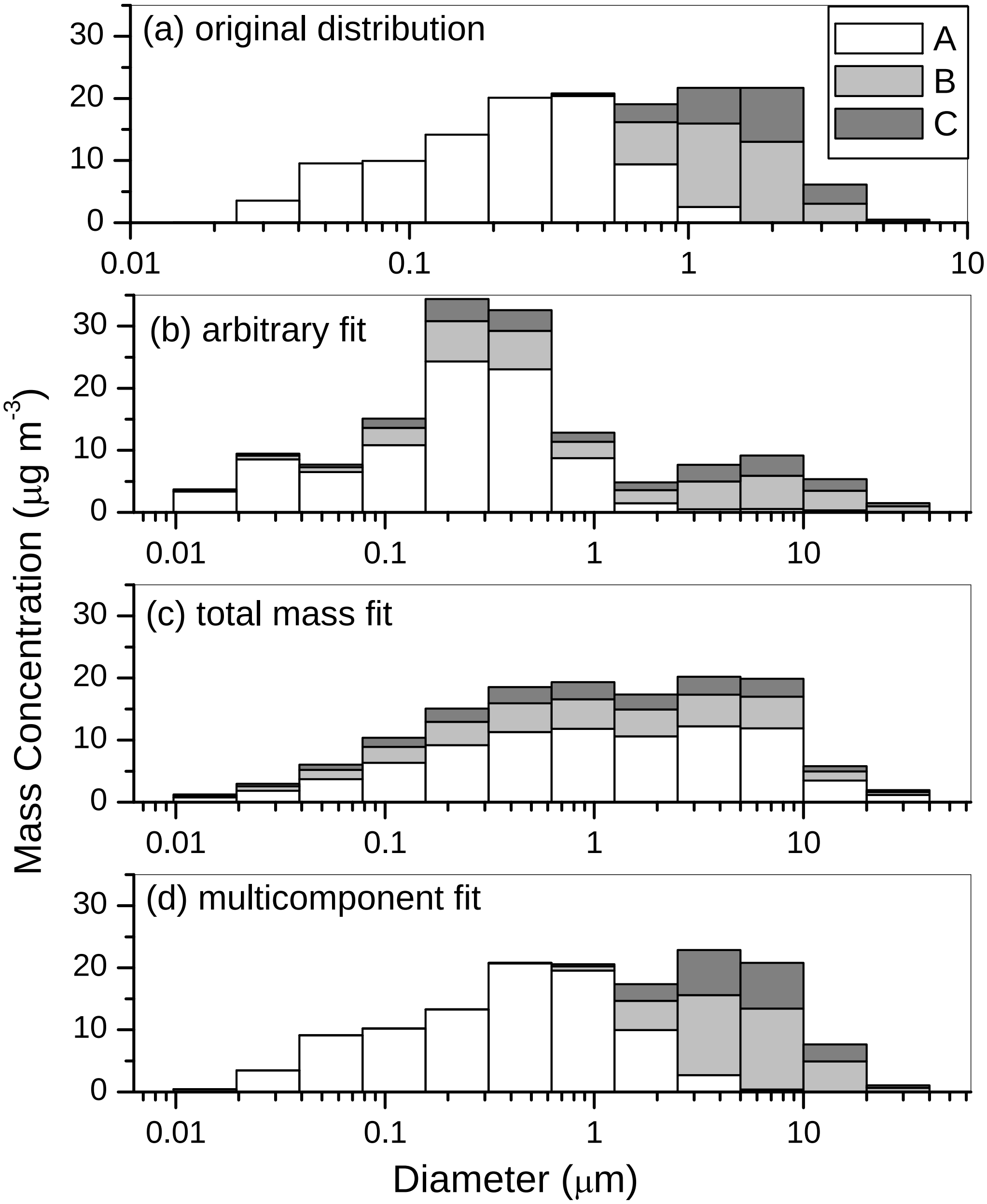

Figure 3.4 Original sectional distribution and sectional distributions created after 5 conversion cycles between sections and modes. (a) original sectional distribution; (b) arbitrary fit; (c) total mass fit; (d) multicomponent fit.

distributions are shown in Figure 3.4 along with the original distribution. When using the multicomponent fit, after the first conversion cycle, which transforms the irregular distribution into lognormal modes, the distribution stays the same. With the total mass fit, the overall size distribution remains constant after the first cycle, but components continue to mix and after 5 iterations all sections have nearly identical composition. For the arbitrary fit, both the overall and individual component distributions continue to change for each iteration, but components do not mix as rapidly as with the total mass fit.

Comparing the overall results for this example distribution, the arbitrary fit method conserves mass, but has difficulty fitting the size and component distributions; the total mass fit method is able to conserve mass and fit the size distribution, but distorts the component distribution; the multicomponent fit method can satisfy all three criteria for a good fit, correctly allocating components in addition to fitting the size distribution and conserving mass. Similar results were obtained in tests with other sectional distributions.

The multicomponent fit also works well at converting distributions with fewer size sections and where the size sections do not span the entire distribution. If a sectional distribution is derived from a perfectly lognormal distribution, it can typically be reproduced exactly. Even for more realistic sectional distributions, that are not exactly lognormal and that contain most but not all of the full particle size range, the multicomponent fit can provide a reasonable modal distribution. An example sectional distribution with 3 distinct peaks and 3 components is shown in Figure 3.5. When all 12 sections (0.01 - 40 µm) are used, the converted modal distribution is an accurate fit of the sectional distribution, as seen in Figure 3.5a. When only 8 sections (0.04-10 µm) are used

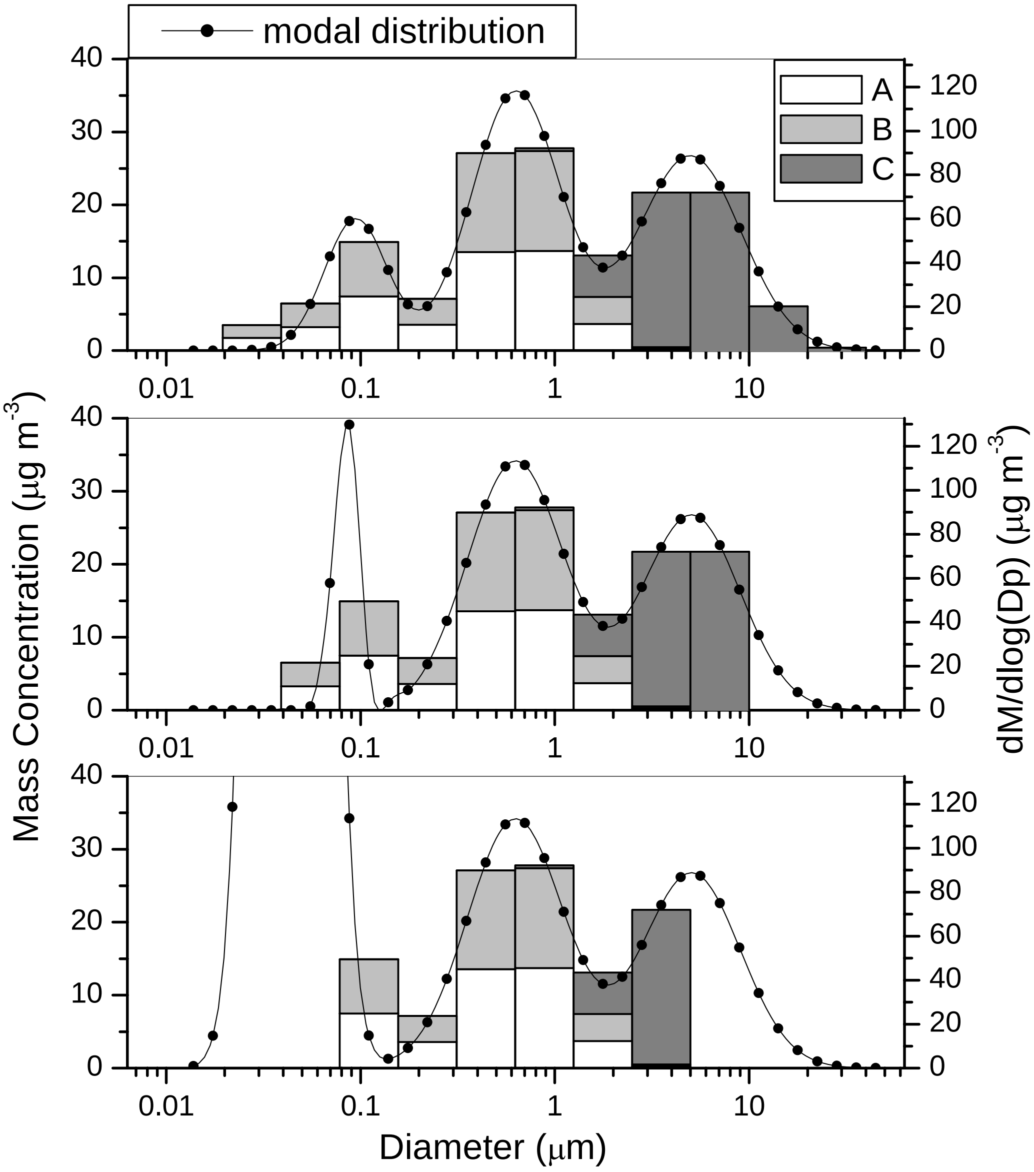

Figure 3.5 Modal distributions created using multicomponent fit method to convert original sectional distribution with (a) 12 sections; (b) 8 sections; (c) 6 sections.

(Figure 3.5b) a modal distribution with 3 modes is also created. The second and third modes are very similar to results with all 12 sections, but the first mode is much narrower when only 8 sections are used. If only 6 sections (0.078-5 μm) are provided (Figure 3.5c), much more sectional information is lost and the converted modal distribution is much less reliable. With only the smallest section indicating the presence of a first mode and no difference in composition distinguishing it from the second mode, a huge nuclei mode is created. Extrapolating beyond the sectional size range in this manner is not recommended. The portion of the distribution within the sectional size range may remain accurate, but trying to create an entire mode outside of the known size range is bound to result in errors.

Conclusions

In this work a new method is presented for converting a multicomponent size distribution from sectional to modal form. A sectional distribution is fit with multiple lognormal modes using a non-linear least square regression that considers both the overall mass distribution and individual component distributions. Results of conversion tests show that the multicomponent fit method is able to define a modal distribution that accurately represents the original sectional distribution. This new method offers much more accurate fits than other approaches that assign sections to modes arbitrarily or that fit only the total mass distribution. These other methods tend to misrepresent the overall size distribution and are subject to compositional diffusion within the distribution. With the multicomponent fit method total and component mass are conserved, the size, shape, and location of peaks match the original distribution, and modal compositions allocate components to the same size range as in the sectional representation. It is also able to convert distributions with relatively few size sections or where the size sections do not span the entire distribution.

CHAPTER IV

DEVELOPMENT AND APPLICATION OF A NEW AEROSOL MODEL FOR INVESTIGATING INTERACTIONS BETWEEN AEROSOL MIXING STATE, SEMIVOLATILE ORGANIC PARTITIONING, AND COAGULATION

Introduction

Aerosol particles in atmosphere have various impacts on human health (Pope 2000), visibility reduction (Blando et al. 1998; Malm and Day 2000), and global climate (Penner et al. 2001). Organic compounds typically constitute from 10% to 70% of the total fine particle mass in both urban and rural areas and have high diversity of components, so organic aerosol is an important part of air pollution problem (Turpin et al. 2000). Organic aerosol can be emitted directly from emission sources, which is named as primary organic aerosol (POA), or formed by condensing of semivolatile organic compounds (SVOC) from gas to particle phase, which is defined as secondary organic aerosol (SOA) (Pandis et al. 1992; Jacobson et al. 2000). In average, SOA comprises 25 – 50% of total organic mass in urban aerosol, and it could be up to 70% in very severe polluted area. Many research works with the concern of SOA formation and distribution have been done, trying to characterize the behavior of organic aerosol (Odum et al. 1996; Bowman et al. 1997; Griffin et al. 1999; Leach et al. 1999; Pankow et al. 2001; Pun et al. 2002; Chandramouli et al. 2003b).

Many studies have shown that aerosol emissions from different sources have distinct compositions (Rogge et al. 1993; Noble and Prather 1996; Gard et al. 1998), so that aerosol particles exist in what is termed an external mixture once emitted. But the mixing state of particles is not constant, they evolve over time. Condensation of semivolatile compounds from gas to particle phase lets different kind of particles have same compounds, and coagulation between different kinds of particles enable components belonging to different emission categories to exist in same particle. As particles interact with each other and the gas phase, they become more compositionally similar and resemble an internal mixture, in which all particles have the same composition. Single particle measurements have helped illuminate this transition from external to internal mixing. Hasegawa and Ohta (Hasegawa and Ohta 2002), for example, found that in urban areas, where emissions sources are nearby, soot particles were externally mixed, but in non-urban areas, where particles had undergone long range transport, internal mixtures of soot and water soluble materials were more common. Naoe and Okada (Naoe and Okada 2001) used the dialysis (extraction) of water-soluble material method to measure soot-containing particles, and found that the number fractions of internally mixed soot particles increased from 34% in Aitken mode (0.03 – 0.1µm), the size range that soot particles were initially emitted, to 67% in the large size range (0.1 – 0.35µm).

Aerosol mixing state can influence the formation of SOA, because gas-aerosol partitioning is affected by the composition of particle phase. For externally mixed particles, the condensation of semivolatile organic compounds from gas to particle phase is different for different kind of aerosol particles, resulting in uneven component distributions. For internal mixture, however, all the particles with same size have same growth rate because of their uniform composition. Assuming an incorrect mixing state can artificially distort the aerosol size and component distribution (FassiFihri et al. 1997; Kleeman et al. 1997; Jacobson 2001b, 2002). As shown in the work of Kleeman et al.

(Kleeman et al. 1997), when Na^+ and SO_4^{2-} are assumed to exist in different particles, an originally monodisperse aerosol distribution developed to a biomodal distribution, a result which is observed in atmospheric measurements, but cannot be reproduced by assuming internal mixture.

Limited by the understanding of aerosol mechanism and computation ability, aerosol particles are assumed as internal mixture in most air quality models (Wexler et al. 1994; Binkowski and Shankar 1995; Jacobson 1997b, a; Meng et al. 1998; Sun and Wexler 1998b; Zhang et al. 2004). Recently, two different approaches for describing and external mixture have been used in models developed by Kleeman (Kleeman et al. 1997; Bhave et al. 2002; Ying et al. 2004) and Jacobson (Jacobson 2001b, 2002). The Kleeman source-oriented external mixture trajectory model represents the aerosol with thousands of particle classes defined according to particle size, source category, and time of emission. These distinct populations interact with the same gas phase, but evolve independently based on their unique compositions. The model does not account for coagulation, however, which was considered to have a negligible effect on aerosol mass distribution for urban time scales. Jacobson's approach describes the aerosol with several single source populations that interact with the gas phase and with each other to form additional mixed composition populations. When coagulation or condensation occurs, mass is transferred to the appropriate mixed distribution. In accounting for coagulation it places all binary mixture into the same distribution, regardless of the relative amounts of each component. As a result, a particle that has 99% A, 1% B and a particle that has 1% A, 99% B will be grouped in the same population of AB mixture.

The focus of this research is to determine the impact of aerosol mixing state on SOA formation. In the following sections, I first present the formulation of new model, detailing a new methodology that is used to define internally and externally mixed particles. Then, the formation of SOA on externally mixed particles in a simplified urban area scenario is simulated, and the more complex composition and size distributions are shown, which can not be obtained when particles begin as an internal mixture. Lastly, the effects of coagulation and criteria definition of particles mixing states on the performance of new model are analyzed.

Model Formulation

Overall Model Framework

A new aerosol box model is constructed for the investigation of interactions between aerosol mixing state, semivolatile organic compounds partitioning, and coagulation, which is formulated in a Lagrangian coordinate system as a trajectory model. In the model, primary organic aerosol (POA) and inorganics are initially presented and continuously emitted into the model cell. Secondary organic aerosol (SOA) is formed by the reaction of an emitted hydrocarbon precursor. Based on emission and meteorological information, the evolution of aerosol size and composition distribution over time is calculated by this aerosol model.

In the model, aerosol particles can be described as external mixture, where different emission sources have different size and composition distributions. A new representation of the aerosol distribution is provided which classifies particles into discrete bins based on both size and composition, with sufficient resolution to distinguish between different compositional mixtures. Because of the mixing of particles and partitioning of semivolatile components between gas and particle phases, new aerosol distributions, with different composition from the initially emitted ones, will be produced. The dynamic processes of aerosol particles in this model include condensation, coagulation, emission and deposition. The model is based on previous aerosol models (Bowman et al. 1997; Sheehan and Bowman 2001; Bowman and Karamalegos 2002; Bowman and Melton 2004), with the calculation of coagulation and gas-to-particle mass transfer updated to account for the new treatments of aerosol distributions and thermodynamics. For coagulation between particles belonging to different size and composition bins, an expanded process, based on the work of Jacobson (Jacobson et al. 1994; Jacobson 2002), for determining to which distribution and bin coagulated particles are assigned based on their composition is added. Gas to particle mass transfer is determined with a dynamic approach that calculates the mass transfer rate between the gas phase and particles in each bin. The moving center sectional method (Jacobson 1997a) is used for condensational growth and is similarly modified to transfer particles to the appropriate compositional bin as they grow in size and change composition.

Definition and Representation of Externally Mixed Particles

Externally mixed particles have different composition and evolution history, and an appropriate separation for size and compositionally resolved aerosol is required. A new sectional approach is developed, where different compositional mixtures are categorized into different populations such that particles are divided into discrete bins based on size and composition. This new scheme is expanded on that used by Jacobson (Jacobson 2001b, 2002) to provide greater compositional detail. The goal is to distinguish between particles that are truly mixed, i.e., containing significant fractions of different components, and ones that, while technically a mixture, contain only small amounts of other components.

In the work of Jacobson, for example, all the particles that come from coagulation are defined as internal mixture. This definition has no problem if the collision particles have similar size. But if the collided two particles with different composition have 100 times difference in diameter, then the mass of smaller particles only account for 10^{-6} in the coagulated particle. It is far from reasonable if the formed particle is still considered as internal mixture. Here I specify a threshold that defines what is considered a significant amount of an individual component. For example, with a 5% threshold, particles would need to be at least 5% A and 5% B to be categorized in the AB population. Particle with 99% A and only 1% B would remain in the "pure" A population. To further illustrate, a ternary system of A, B and C will use the compositional categories depicted in Figure 4.1.

In a general definition of this compositional distribution structure, the total number of possible aerosol distributions, N_d, is determined by the number of particle phase components, N_c, according to:

$$N_d = 2^{N_c} - 1 \tag{4.1}$$

The index number, m (m=1, … N_d), of each particle population's distribution is defined as:

$$m = \sum_{i=1}^{N_c} f(i) * 2^{i-1} \tag{4.2}$$

where $f(i)$ is a binary number, indicating if the mass fraction of component i, $x(i)$, exceeds the specified mixing threshold criterion, c, with $c \leq 1/N_c$, according to:

$$f(i) = \begin{cases} 1 & \text{when} \quad x(i) > c \\ 0 & \text{when} \quad x(i) < c \end{cases} \tag{4.3}$$

This definition gives a reasonable representation of mixed particles and still limits the type of aerosol particles to countable numbers. Impacts of the definition of different threshold values on the evolution of externally mixed particles are analyzed in my research, and an optimized value is provided.

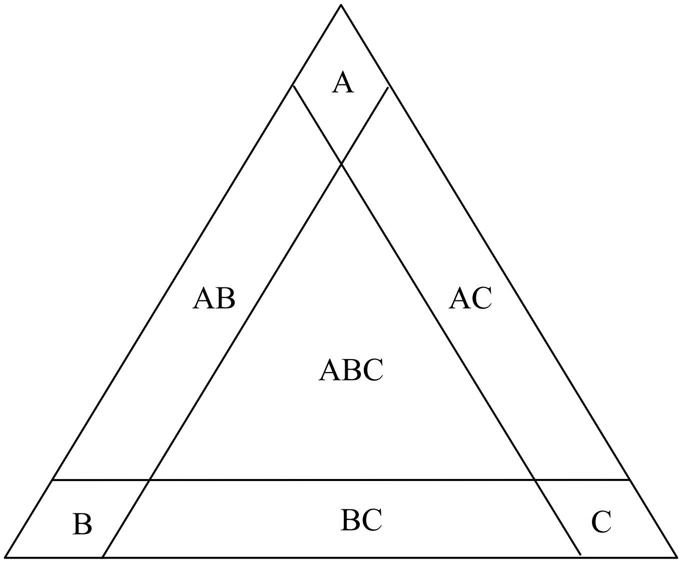

Figure 4.1 Compositional categories for a ternary aerosol system.

Gas-to-particle Conversion and SOA Formation

The partitioning of SOA is represented by an absorption mechanism, where gas phase semivolatile products partition into an existing aerosol phase of absorbing material (Pankow 1994; Odum et al. 1996). Absorptive partitioning of a semivolatile compound *i* is described by a partitioning coefficient K_i,

$$K_i = \frac{F_i}{C_i * M_o} \tag{4.4}$$

where K_i is a temperature-dependent equilibrium partitioning constant; F_i and C_i are the mass concentrations of semivolatile species *i* in the particle and gas phases, respectively; and M_o is the concentration of absorbing aerosol. Following the work of Pankow (Pankow 1994) the absorptive partition coefficient can be expressed as a function of physical and thermodynamic properties of the semivolatile compound

$$K_i = \frac{RT}{MW \xi_i p_i^o} \tag{4.5}$$

where *R* is the gas constant, *T* is temperature, *MW* is the mean molecular weight of the absorbing aerosol phase, ζ_i is the activity coefficient of compound *i* in aerosol phase, and p_i^0 is the vapor pressure of compound *i* as a liquid.

K_i values are not constant, but vary with temperature and aerosol composition (Odum et al. 1996; Pankow et al. 2001; Chandramouli et al. 2003a). The activity coefficient, ζ_i, in equation (4.5) reflects the interaction of aerosol component *i* with the remaining absorbing aerosol mixture, which may contain inorganic compounds, semivolatile and nonvolatile organics. As a result, the partitioning of semivolatile organics is dependent on the composition of the absorbing aerosol phase present in the atmosphere.

Fully dynamic mass transfer method is used for gas-particle transport (Meng and Seinfeld 1996; Meng et al. 1998; Sun and Wexler 1998a; Pilinis et al. 2000). The driving force for mass transfer of a semivolatile component *i* is the difference between the bulk gas phase concentration and the gas phase concentration in equilibrium with a given aerosol phase. The mass flux of a semivolatile compound *i* to a single aerosol particle can be written as:

$$J_i = 2\pi D_p D_i \frac{C_{i,\infty} - C_{i,eq}}{\dfrac{2\lambda}{\alpha_i D_p} + 1} \tag{4.6}$$

where D_p is particle diameter, D_i is the diffusivity of species *i*, λ is the air mean free path, and α_i is the accommodation coefficient of species *i* on the particle. $C_{i,\infty}$ is the concentration of *i* in the bulk gas phase, and $C_{i,eq}$ is the gas-phase concentration in equilibrium with the aerosol particle, which is derived from equation (4.4):

$$C_{i,eq} = \frac{F_i}{K_i * M_o} \tag{4.7}$$

where K_i is the absorption partitioning coefficient, which is defined by equation (4.5). Vapor pressures of the SOA components, p_i^0, in equation (4.5), are determined as a function of temperature according to the Clasius-Clapeyron equation (Atkins 1990)

$$p_i^0(T) = p_i^0(T^*)\exp\left[-\frac{H_i}{R}\left(\frac{1}{T} - \frac{1}{T^*}\right)\right] \tag{4.8}$$

where $p_i^0(T)$ is the vapor pressure of component *i* at temperature *T*, $p_i^0(T^*)$ is the vapor pressure of component *i* at reference temperature T^*, and H_i is the enthalpy of vaporization of component *i*. Activity coefficients, ζ_i, in equation (4.5), are determined using the UNIFAC group contribution method (Fredenslund et al. 1975). It calculates activity coefficients based on aerosol phase composition, x_i, and the number of functional groups of type j in each molecule i, s_{ji}.

$$\xi_i = f(x_i, s_{ji}) \tag{4.9}$$

Thus, to calculate partitioning coefficients, $p_i^0(T^*)$, H_i, MW_i, and s_{ji} are specified for each semivolatile organic aerosol component.

Since the focus of current study is the formation of SOA, the representation of inorganic components is highly simplified. In the model, inorganics are assumed to be inert and nonvolatile with no partitioning between gas and particle phase. One general compound is used to represent all the inorganic components. In the particle phase, there are no interactions between inorganic and organic components, and the inorganic doesn't change the properties of organic components. But the existing of inorganic may change the distribution to which a particle belongs through altering the concentration of each component in particle phase. With the further understanding of interaction between inorganic and organic compounds in particle phase (Liang et al. 1997; Griffin et al. 2002a; Koo et al. 2003), inorganic partitioning can be added to the model for the situations where the effects of inorganic could not be neglected.

Coagulation

Coagulation is an important process for urban aerosols, which is dominated by smaller size particles with high number concentration, by changing their composition and size distributions. Through decreasing the number and increasing the size of particles, coagulation process mixes the particles with different size and composition, inducing the alteration of particles mixing states.

Different from the coagulation of internal mixture, which has only one distribution, the coagulation process is much more complex for externally mixed particles. For coagulation process of internally mixed particles, we only need to find which section the coagulated particle belongs to. But for externally mixed particles, the coagulated particle may have different composition from the colliding particles, so we need to find not only the section where the coagulated particle should be located based on its size, but also the distribution where the particle belongs based on its composition.

The coagulation equation for a monomer sectional aerosol distribution, where the volume of particle in section *k* is *k* times the volume of particle size in section 1, can be written in finite difference form as (Jacobson et al. 1994; Seinfeld and Pandis 1998):

$$\frac{n^t(k)-n^{t-1}(k)}{\Delta t}=\frac{1}{2}\sum_{j=1}^{k-1}\beta(k-j,j)n^t(k-j)n^t(j)-\sum_{j=1}^{\infty}\beta(k,j)n^t(k)n^t(j) \qquad (4.10)$$

where $n^t(k)$ is the time-dependent number concentration of particle in section k at time t, β is the coagulation kernel, or collision rate, of two colliding particles, and Δt is the time step. Equation (4.10) can be rewritten in terms of $n^t(k)$ as:

$$n^t(k)=\frac{n^{t-1}(k)+\frac{1}{2}\Delta t\sum_{j=1}^{k-1}\beta(k-j,j)n^t(k-j)n^t(j)}{1+\Delta t\sum_{j=1}^{\infty}\beta(k,j)n^t(j)} \qquad (4.11)$$

For general multicomponent sectional aerosol distribution with an arbitrary size bin structure, the coagulation equation can be written in terms of volume concentration as (Jacobson et al. 1994; Jacobson 1997c):

$$v_q^t(k)=\frac{v_q^{t-1}(k)+\frac{1}{2}\Delta t\sum_{j=1}^{k}\sum_{i=1}^{k-1}f(i,j,k)\beta(i,j)v_q^t(i)n^t(j)}{1+\Delta t\sum_{j=1}^{N_S}(1-f(k,j,k))\beta(k,j)n^t(j)} \qquad (4.12)$$

where $v^t_q(k)$ is the time-dependent volume concentration of component q of particle in section k at time t. With the colliding of two particles of size v_i and v_j, the coagulated particle has volume $V=v_i+v_j$, which may not equal the characteristic volume of particles in section k, u_k. For the volume-conserving of coagulation calculation, this intermediate particle is divided between section k and $k+1$, and a volume fraction $f(i,j,k)$ is defined to represent this partition (Jacobson et al. 1994; Jacobson 1997c):

$$f(i,j,k)=\begin{cases} \left(\dfrac{u_{k+1}-V}{u_{k+1}-u_k}\right)\dfrac{u_k}{V} & u_k \le V < u_{k+1} \qquad k<N_S \\ 1-f(i,j,k-1) & u_{k-1}<V<u_k \qquad k>1 \\ 1 & V \ge u_k \qquad k=N_S \\ 0 & all \quad other \quad cases \end{cases} \tag{4.13}$$

And further, for externally mixed particles with multicomponent sectional size distribution, the coagulation equation for two colliding particles, one from section i in distribution Na and one from section j in distribution Nb, can be written as:

$$v_q^t(Nc,k)=\frac{v_q^{t-1}(Nc,k)+\frac{1}{2}\Delta t\sum_{Na=1}^{N_T}\sum_{Nb=1}^{N_T}\sum_{j=1}^{k}\sum_{i=1}^{k-1}f(Na,i,Nb,j,Nc,k)\beta(Na,i,Nb,j)v_q^t(Na,i)n^t(Nb,j)}{1+\Delta t\sum_{Nb=1}^{N_T}\sum_{j=1}^{N_S}(1-f(Nc,k,Nb,j,Nc,k))\beta(Nc,k,Nb,j)n^t(Nb,j)} \tag{4.14}$$

and the number concentration is updated as:

$$n^t(Nc,k)=\frac{\sum_{q=1}^{N_Q}v_q^t(Nc,k)}{u_{Nc,k}} \tag{4.15}$$

where N_T ,N_S and N_Q are the total number of distribution, sections and components in each distribution, respectively. $v^t_q(Nc,k)$ is the volume concentration of component q of coagulated particle in section k belonging to distribution Nc at time t. $v^t_q(Na,i)$ is the volume concentration of one colliding particle, which is from section i in distribution Na, at time *t*. n^t *(Nb,j)* is the number concentration of another colliding particle, that comes from section *j* in distribution *Nb*, at time *t*. *β(Na,i,Nb,j)* is the coagulation kernel of two colliding particles, and *f(Na,i,Nb,j,Nc,k)* is the volume fraction of coagulated particle to section *k* in distribution *Nc*, because of the coagulation of two particles from section *i* in distribution *Na* and section *j* in distribution *Nb*. This definition can be further expended from equation (4.13):

$$f(Na,i,Nb,j,Nc,k)=\begin{cases}\left(\dfrac{u_{Nc,k+1}-V_{Na,i,Nb,j}}{u_{Nc,k+1}-u_{Nc,k}}\right)\dfrac{u_{Nc,k}}{V_{Na,i,Nb,j}} & u_{Nc,k}\le V_{Na,i,Nb,j}<u_{Nc,k+1} \quad k<N_S\\ 1-f(Na,i,Nb,j,Nc,k-1) & u_{Nc,k-1}<V_{Na,i,Nb,j}<u_{Nc,k} \quad k>1\\ 1 & V_{Na,i,Nb,j}\ge u_{Nc,k} \quad k=N_S\\ 0 & all \quad other \quad cases\end{cases} \tag{4.16}$$

where $V_{Na,i,Nb,j}=u_{Na,i}+u_{Nb,j}$, is the total mass of collided particle, and $u_{Nc,k}$ is the characteristic volume of a single particle in section *k* belonging to distribution *Nc*.

To perform a coagulation calculation, first, the distribution index number of coagulated particle (*Nc*) is calculated, based on the combined composition of the two colliding particles. Then the coagulated particle is relocated to the corresponding sections in this distribution based on equation (4.15). Unlike the work of Jacobson (Jacobson et al. 1994; Jacobson 2002), where the coagulated particles can only be moved from external mixture to internal mixture, the externally mixed particles can also be moved back to internal mixture, such as when a very small size internally mixed particle collides with a large size externally mixed particle, the newly coagulated particle belongs to external mixture. So, the semi-implicit coagulation method used by Jacobson where the number concentration at time *t* can be substituted by the value of time *t-1*, because externally mixed distributions can be calculated before internally mixed distributions, allowing for a non-iterative solution, can not be used in our coagulation system.

Instead, an iterative method is used to solve the explicit coagulation equations (4.14). As shown in equation, to calculate $v^t_q(Nc,k)$, the volume and number concentration of particles in all other sections will be needed and even with a semi-implicit approach the set of equations would need to be solved simultaneously. During the calculation of iteration method, the volume and number concentration for each section are updated by equations (4.14) and (4.15) using volume and number concentrations from the previous iteration. Values from the previous time step are used as initial guesses for the first iteration. Iterations are continued until the relative difference of volume concentration between two consecutive iterations is less than 0.1% for all particles. The value of criterion for iteration termination was selected to provide a balance of accuracy and calculation speed for this specific system. Different systems may require other values of the criterion.

Emission

A wide range of primary organic compounds and semivolatile organic compounds with diverse polarity and vapor pressure have been detected in urban atmosphere. Some of them are produced by the photochemical reactions happened in gas phase, others are emitted directly from various emission sources. In the model, emission process includes the emission of primary particles and the release of precursors of semivolatile organic compounds in gas phase. All the primary particles are emitted as external mixtures, that is to say, particles from one source have the same composition among the whole distribution range, but are different from the particles of other sources. The emission rate of gaseous precursors controls the concentration of semivolatile organic compounds in gas phase, influencing the rate of SOA formation.

Deposition

In this Lagrangian model, deposition is the only process of removing aerosol particles from trajectory cell. The dry deposition velocity of a particle may be written as (Seinfeld and Pandis 1998):

$$v_d = \frac{v_s}{\left[1 - \exp\left(-(r_a + r_b) * v_s\right)\right]} \tag{4.17}$$

where v_d is particle deposition velocity, v_s is particle gravitational settling velocity which increases with particle size, r_a is aerodynamic resistance, and r_b is quasi-laminar resistance. The detailed explanation can be found in Seinfeld and Pandis (1998) and CMAQ model (Binkowski 1999; Binkowski and Roselle 2003).

Since v_d is related to the size of particles, deposition losses will vary for different size sections. The earth surface has a high resistance to smaller size particles, so larger size particles deposit faster than smaller ones. Once we calculate the falling length of particles by the deposition velocity and time step, the number ratio of particles of a given size that fell to ground is determined by comparing falling length to the model cell height and the number of particles in different sections is updated.

Model Simulation

Base case scenario

For the purpose of investigating interactions between aerosol mixing states, SOA partitioning, and coagulation, a base case air pollution scenario is constructed with the information of ambient air and meteorological conditions, and gas and particles emission. Because there are large amount of emission sources and variations of semivolatile organic compounds, urban and regional area is the concern of most air quality research (Lawson 1990; Solomon et al. 2003). The base case scenario is constructed based on a simplified urban episode, where the concentration of fine particles is approximately 60µg m^{-3}, with around 50% organic and 50% inorganic compounds. In order to have a full evolution history of all particles, the system is simulated as long as 8 days. The ambient temperature varies hourly with time every day, ranging from 15 to 35 ^{o}C. The mixing height is set as 1250 meter, and the particles are assumed well mixed along the whole height.

The components used in the simulation are listed in Table 4.1, together with their properties. PO1 and PO2 are emitted as primary organic aerosol, with low and high polarity respectively. The more nonpolar primary organics, PO1, are represented by heneicosane, a long chain alkane with 21 carbons typical of diesel soot; the more polar primary organics, PO2, are represented by levoglucosan, a key component of smoke particles with multiple hydroxyl and ether groups. SV1 and SV2 represent semivolatile organic compounds of low and high polarity. With lower polarity, SV1, represented by eicosanoic-acid, is a long chain acid with 20 carbons, and SV2, represented by pinic-acid, with higher polarity, has two carboxyl and two ethylene groups. The emission of other components is represented by INERT, which will change the size and composition of particles but doesn't affect the partitioning of SOA. Initially, there are only PO1, PO2 and INERT existing in the model volume. SV1 and SV2 are produced in the gas phase at equal rates, and condensed to particle phase by partitioning thereafter. During the simulation process, there are constant emission rates of PO1, PO2 and INERT, with daily emission rates of 10.8, 10.8 and 43.2 μg m^{-3}, respectively.

Table 4.1 Properties of compounds in particle phase.

Symbol	Name	K	Hvap	MW	Polarity
PO1	Heneicosane	1.0E+12	0.0	296	Low
PO2	Levoglucosan	1.0E+12	0.0	162	High
SV1	Eicosanoic-acid	7.23E-2	17.9	312	Low
SV2	Pinic-acid	6.10E-2	17.9	186	High
INERT					

* K (m^3 μg^{-1}), partitioning coefficient; Hvap (kcal mol^{-1} K^{-1}), heat of vaporization; MW (g mol^{-1}), molecular weight.

Aerosol particles can be set as either internal or external mixture during simulation. For internal mixture, there is only one aerosol distribution, where the emission of PO1, PO2 and INERT can be seen as from one emission source. The size and composition of this single distribution evolved during simulation process, with the partitioning of SV1 and SV2, coagulation between particles, and deposition to ground surface. If set as external mixture, PO1, PO2 and INERT are emitted from 3 emission sources with 3 aerosol distributions of different composition. During the evolution of particles, because of partitioning of SV1 and SV2 between gas and particle phase, and the coagulation between particles, the composition of initial 3 distributions will be changed.

Based on the definition of external mixture, some new distributions will be produced. Since 5 compounds are found in the simulation system, there are a total of 31 ($=2^5-1$) possible distributions. In this base case scenario, the mixing threshold criterion, *c*, is set at 0.1, which means a compound is considered part of a mixture only when there is at least 10% mass of this compound among the total particle mass. The choosing of criterion value will be discussed in section 4.3.4. No matter which kind of mixing state of particles is used, each distribution is represented by moving center sectional method, with 10 sections, logarithmically spaced from 0.01 to 2.5 μm.

The parameters for initial and emission sectional distributions of PO1, PO2 and INERT are listed in Table 4.2, and Figure 4.2(a) shows the plot of initial sectional distribution. When aerosol particles exist as internal mixture, there is only one single distribution well mixed by PO1, PO2 and INERT in each section, with peak at 0.09 μm. When particles are externally mixed, the sectional distribution in Figure 4.2 (a) is actually composed of three individual distributions composed by pure PO1, PO2 and INERT, respectively, with the same total mass and components distributions as internal mixture.

Comparison of external and internal mixture results

Base case scenario are simulated for both externally and internally mixed particles, with same meteorological conditions, emission of gas and particles, and concentrations of ambient semivolatile compounds. The simulated components and size distributions of both external and internal mixture are illustrated in Figure 4.2, and the parameters of each distribution are shown in Table 4.3.

Table 4.2 Parameters for initial and emission sectional distribution of PO1, PO2 and INERT.

Section	Diameter (μm)	Initial Distribution ((μg m^{-3})			Emission Rates (μg m^{-3} hr^{-1})		
		PO1	*PO2*	*INERT*	*PO1*	*PO2*	*INERT*
1	0.02	4.8E-4	4.8E-4	0.002	7.2E-5	7.2E-5	2.9E-4
2	0.034	0.058	0.058	0.233	8.7E-3	8.7E-3	0.035
3	0.058	0.881	0.881	3.526	0.132	0.132	0.529
4	0.1	1.660	1.660	6.640	0.249	0.249	0.996
5	0.171	0.389	0.389	1.555	0.058	0.058	0.233
6	0.292	0.011	0.011	0.045	1.7E-3	1.7E-3	6.8E-3
7	0.5	4.1E-5	4.1E-5	1.6E-4	6.1E-6	6.1E-6	2.4E-5
8	0.855	1.8E-4	1.8E-4	7.4E-8	2.8E-9	2.8E-9	1.1E-8
9	1.462	0.000	0.000	0.000	0.000	0.000	0.000
10	2.5	0.000	0.000	0.000	0.000	0.000	0.000

Table 4.3 Comparison of simulation results of externally and internally mixed particles. With 8 days simulation and 10% criterion.

	External Mixture	Internal Mixture
Total number (# cm^{-3})	4.991E+04	5.809E+04
Total mass (μg m^{-3})	59.5	61.4
Inert (μg m^{-3})	28.5	28.7
Organic (μg m^{-3})	31.1	32.7
PO1 (μg m^{-3})	6.58	7.18
PO2 (μg m^{-3})	7.10	7.18
SV1 (μg m^{-3})	10.7	11.6
SV2 (μg m^{-3})	6.67	6.71

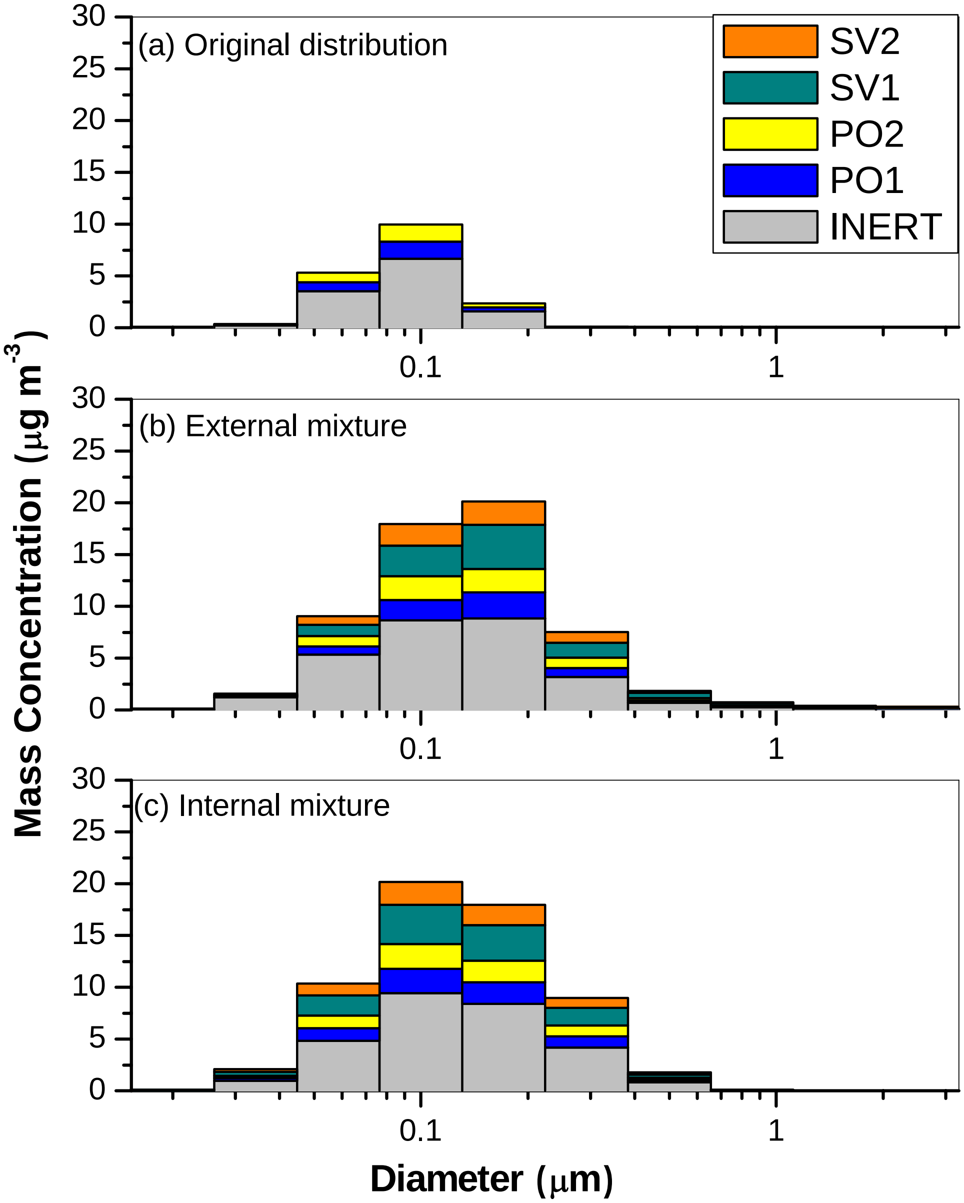

Figure 4.2 Distribution of externally and internally mixed particles from same origin. (a) initial distribution, (b) external mixture, (c) internal mixture.

Because of their polarity, nonpolar SV1 prefers to condense on particles composed of nonpolar PO1, while polar SV2 is more likely to partition to polar PO2 particles. When particles are treated as internal mixture, this partitioning difference between SV1 and SV2 is not seen, because all the particles have same percentage of PO1 and PO2. As a result, for an internal mixture particles with different size have same percentage of all kinds of components, which is shown in Figure 4.2(c). Because SV1 has a higher partitioning coefficient, more SV1 condenses to particle phase than SV2, and there is a higher percentage of SV1 in each section.

But things are different for externally mixed particles. Because more SV1 condenses to particle phase than SV2, and SV1 partitions preferentially to PO1, particles made of PO1 grow faster than those of PO2. As a result, the composition is not evenly distributed in all size particles at all. The detailed component distribution in each section is shown in Table 4.4, with accompanying pie plots of composition for corresponding particles. As illustrated in the table, higher percentages of PO1 and SV1 in particle phase occur with the increasing of size. Because the growth of PO2 is well behind PO1, the highest percentage of PO2 and SV2 exists in the middle of sectional distribution. INERT is the component mostly in smaller size particles since no semivolatile organic components condense on it, and the movement of INERT to larger size particle is only based on coagulation between particles.

A much broader aerosol size distribution is another difference of externally mixed particles from internal mixture, which is shown in Figure 4.2. The faster growth rate of particles made by PO1 and the coagulation involving these larger particles result in a significant amount of particles in the largest three sections. Large size particles have a

Table 4.4 Detailed components distribution of externally mixed particles

Section	Diameter (μm)	Total mass (μg m^{-3})	Component mass (μg m^{-3})					Plots
			PO1	PO2	SV1	SV2	INERT	
1	0.02	0.063	0.000	0.005	0.000	0.003	0.055	
2	0.034	1.552	0.049	0.131	0.072	0.098	1.202	
3	0.058	9.056	0.771	1.003	1.121	0.824	5.338	
4	0.1	17.936	1.956	2.322	2.96	2.049	8.649	
5	0.171	20.145	2.504	2.267	4.276	2.270	8.828	
6	0.292	7.541	0.867	1.003	1.422	1.067	3.183	
7	0.5	1.847	0.247	0.212	0.502	0.207	0.679	
8	0.855	0.728	0.097	0.082	0.201	0.079	0.269	
9	1.462	0.37	0.048	0.041	0.095	0.039	0.147	
10	2.5	0.287	0.037	0.031	0.073	0.030	0.116	

* 🟦 PO1; 🟥 PO2; 🟨 SV1; 🟩 SV2; 🟪 INERT

higher deposition rate, inducing to less number and mass of particles. As shown in Table 4.3, the total number of particles is 4.99*10^4 (# cm^{-3}) and the total mass is 59.5 (μg m^{-3}) for external mixture, comparing to 5.81*10^4 (# cm^{-3}) and 61.4 (μg m^{-3}) in internal mixture, respectively. The most difference exists in the mass of PO1 and SV1, while INERT has least difference between external and internal mixture. This result is correspondent with the analysis of the growth of different particles.

Unlike internally mixed particles, where there is only 1 distribution, there are 10 major distributions, with the number concentration larger than 10 cm^{-3} and more than 0.1 μg m^{-3} of mass concentration, in externally mixed particles, as a result of semivolatile organic components partitioning and coagulation between particles. The detailed composition, mass and number concentrations of each distribution are shown in Table 4.5, with accompanying composition plots.

SOA partitioning and coagulation between particles affect the original 3 distribution in different ways. The original PO1 distribution is disappeared, and most PO1 goes to distribution 1 (PO1/SV1 mixture) because of condensation of SV1, and distribution 6 (PO1/SV1/INERT mixture) due to condensation of SV1 and coagulation with INERT particles. Similarly, there is no PO2 distribution, and most PO2 goes to distribution 2 (PO2/SV2 mixture) and 8 (PO2/SV2/INERT mixture). However, the INERT distribution, distribution 4, still exists with large amount of mass and number concentrations. Because of large amount and constant emission of INERT particles, coagulation, which affects particles distribution on long time range, can not completely transfer all INERT to other distributions.

Table 4.5 Major distributions included in externally mixed particles after simulation.

Index	Composition					Mass (μg m^{-3})	Number (# cm^{-3})	Plots*
	PO1	PO2	SV1	SV2	INERT			
1	+		+			5.412	6131	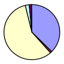
2		+		+		3.368	5589	
3	+	+	+	+		0.629	410	
4					+	19.717	30936	
5			+		+	0.339	76	
6	+		+		+	12.973	3171	
7	+	+	+		+	0.396	11	
8		+		+	+	11.388	3183	
9	+	+		+	+	0.374	91	
10	+	+	+	+	+	4.689	269	

* 🟦 PO1; 🟥 PO2; 🟨 SV1; 🟩 SV2; 🟪 INERT

One particle has the ability to collide with all the others not matter the composition, so some other distributions are also produced, such as distribution 10 (PO1/PO2/SV1/SV2/INERT), 3 (PO1/PO2/SV1/SV2), and so on. Since particles of these distributions are not from original pure distributions, there are less mass and number concentrations. As mentioned previously, as many as 31 distributions could be produced in theory, but in these simulations the other distributions have too small mass and number concentration to be listed in Table 4.5.

Comparison of coagulation effects on size and component distribution of externally and internally mixed particles

Both internally and externally mixed particles are simulated with and without coagulation process, with the same ambient air and meteorological conditions, and gas and particles emissions defined as in base case scenario. The detailed particle phase mass and number concentrations after simulation are shown in Table 4.6, and Figure 4.3 gives the plots of size and components of all distributions.

When coagulation process is not included in our model system, internally and externally mixed particles have not only the same components concentration but also the same total mass concentration. But external mixture has fewer total number concentration as $1.4*10^5$ (# cm^{-3}) than that of internal mixture as $1.8*10^5$ (# cm^{-3}), indicating a faster growth rate of particles in external mixture, though both distributions don’t have a significant growth of particle size, comparing with the initial distribution, as shown in figure 4.2(a). There are much higher peaks of both aerosol distributions, but the peaks are still at around 0.1μm and most particles have diameters less than 0.3μm. The most

Table 4.6 Comparison of simulation results of externally and internally mixed particles with and without coagulation process. With 8 days simulation and 10% criterion.

	Externally Mixed Particles		Internally Mixed Particles	
With coagulation	Yes	No	Yes	No
Total number (# cm^{-3})	4.991E+04	1.399E+05	5.809E+04	1.823E+05
Total mass (μg m^{-3})	59.5	61.5	61.4	61.5
Inorganic (μg m^{-3})	28.5	28.7	28.7	28.7
Organic (μg m^{-3})	31.1	32.8	32.7	32.7
PO1 (μg m^{-3})	6.58	7.18	7.18	7.18
PO2 (μg m^{-3})	7.10	7.18	7.18	7.18
SV1 (μg m^{-3})	10.7	11.7	11.6	11.6
SV2 (μg m^{-3})	6.67	6.80	6.71	6.71

difference of external and internal mixture is the components distribution. Not as in internal mixture, where there is an even distribution of all 5 components in all sections, each section has different composition of externally mixed particles. With the partitioning of SV1 and SV2 between gas and particle phase, the particles made by PO1 and PO2 grew to larger particles, while particles made by INERT stayed in the original position without the condensation of semivolatile organic components. As shown in Figure 4.3 (c), section 2 is dominated by component INERT of external mixture, but the same section of internal mixture has same composition as all the other sections, showing in Figure 4.3(d). Compared with the simulation results where there is no coagulation process, when coagulation is included in our system, both externally and internally mixed particles show different component and size distributions. For internal mixture, when coagulation is included, the total number concentration decreases to $5.8*10^4$ (# cm^{-3}) from $1.8*10^4$ (# cm^{-3}), but there are same components and mass concentration as the results without

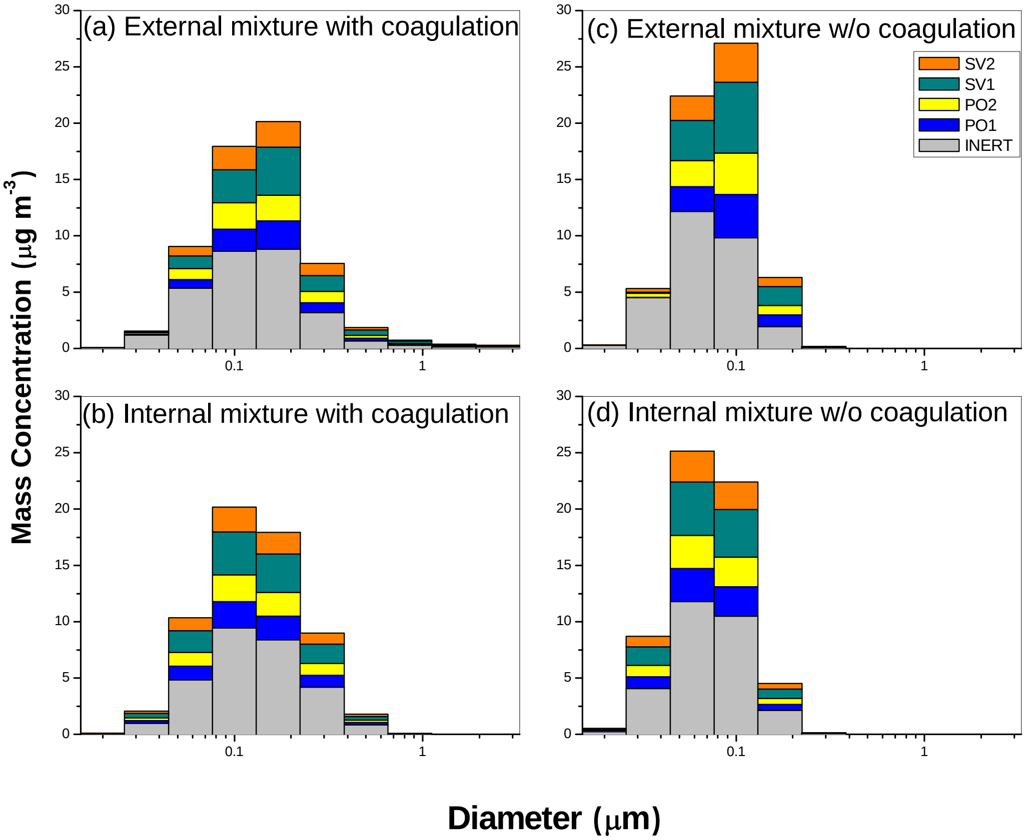

Figure 4.3 Size and components distribution of externally and internally mixed particles after 8 days simulation using *c*=0.1. (a) external mixture with coagulation, (b) internal mixture with coagulation, (c) external mixture without coagulation, (d) internal mixture without coagulation.

coagulation, showing in Table 4.6. Figure 4.3(b), from internally mixed particles with coagulation, shows a much broader distribution comparing to Figure 4.3(d), and there is large number of particles with diameter larger than 0.3μm.

Similarly, for externally mixed particles, because of the coagulation of particles, the total number concentration decreases from $1.4*10^5$ (# cm^{-3}) to $5.0*10^4$ (# cm^{-3}), and there is a much broader distribution, as shown in Figure 4.3(a). Affected by both condensation and coagulation, some particles move further to the largest 3 sections with diameter larger than 1.0μm. Because of the faster deposition speed of large size particles, more aerosol particles are removed from air, inducing a less total mass concentration. As shown in Table 4.6, most loss of mass comes from component PO1 and SV1, where there is a faster growth rate of PO1 than PO2 with more condensation of SV1 than SV2. Through coagulating with other particles, INERT does not only stay in small size particles. But the effect of coagulation on INERT distribution is limited, that the concentration of INERT in larger size particles is so small that the removing of INERT by deposition is neglected, and there is no difference of INERT concentration no matter coagulation is included or not.

Another difference between the simulation results with or without coagulation is the total number of distributions. For internal mixture, there is always only one distribution with same composition for all sections. But for externally mixed particles, as discussed in last section, because of condensation and coagulation, there are totally 10 externally mixed particle distributions with significant amount of particles with different composition. When coagulation process is not included, there are no interactions between different kinds of particles. Then, there are only 3 distributions, which are originated from the initial 3 distributions, and the detailed information is shown in Table 4.7. Since more SV1 is condensed to PO1 particle than SV2 condensing to PO2 particle, distribution 1, composed by SV1 and PO1, has more total mass than distribution 2, made by SV2 and PO2, and distribution 3 is only composed by INERT.

Table 4.7 Distributions included in externally mixed particles after simulation without coagulation.

Index	Composition					Mass ($\mu g\ m^{-3}$)	Number ($\# cm^{-3}$)	Plots*
	PO1	PO2	SV1	SV2	INERT			
1	+		+			19.192	2.32E+04	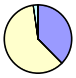
2		+		+		13.624	2.32E+04	
3					+	28.751	9.36E+04	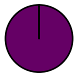

* 🟦 PO1; 🟥 PO2; 🟨 SV1; 🟩 SV2; 🟪 INERT

Sensitivity analysis of mixing criterion

In the base case simulations, 0.1 was arbitrarily defined as the threshold for determining whether a component should be considered part of a mixture. In order to investigate the influence of this mixing threshold on simulation results, the base case scenario was simulated with the mixing threshold criterion, *c*, set as 0.02, 0.05, 0.1 and 0.2, and the simulated aerosol size and composition distributions are compared.

Figure 4.4 gives the plots of size and compositional distributions of externally mixed particles with different mixing criteria. Similar aerosol size and compositional distributions are shown for all plots, where high percentage of INERT is in smaller size particles while the large size particles have higher fraction of organic components. But, the individual mixture mass distributions with different mixing criteria are different, and the distribution with smaller mixing criterion value has faster growing speed. The distribution with the smallest mixing threshold, *c*=0.02 (Figure 4.4a) has a mass peak near 0.17 μm, while for the largest mixing threshold, *c*=0.2 (Figure 4.4d), the peak is near 0.1 μm. Additionally, as the mixing criterion increases, the distribution becomes broader, and there is a significant amount mass concentration in the largest 3 sections for the distribution using *c*=0.2.

As shown in Table 4.8, the definition of mixing criterion has great effects on the number, type and size of the individual distributions, composing each externally mixed distribution. The composition and mass concentration of the main distributions included by each externally mixed distribution with different mixing criterion are shown in Table 4.8. When *c* is set as only 0.02, distribution 7 (mixture of all five compounds) has the highest mass concentration, which is the result of both effects of coagulation and condensation of SVOCs. For increasing values of *c*, the mass concentrations of mixture distributions decrease, because of the higher threshold for defining what constitutes a mixture. When the threshold is as high as 0.2, there are only 3 externally mixed distributions with significant mass concentration. The majority of particle mass is found in distribution 4 (the "pure" INERT mixture), which has a mass concentration of 37.3 μg m^{-3}, as compared to 12.3 μg m^{-3} when *c*=0.02.

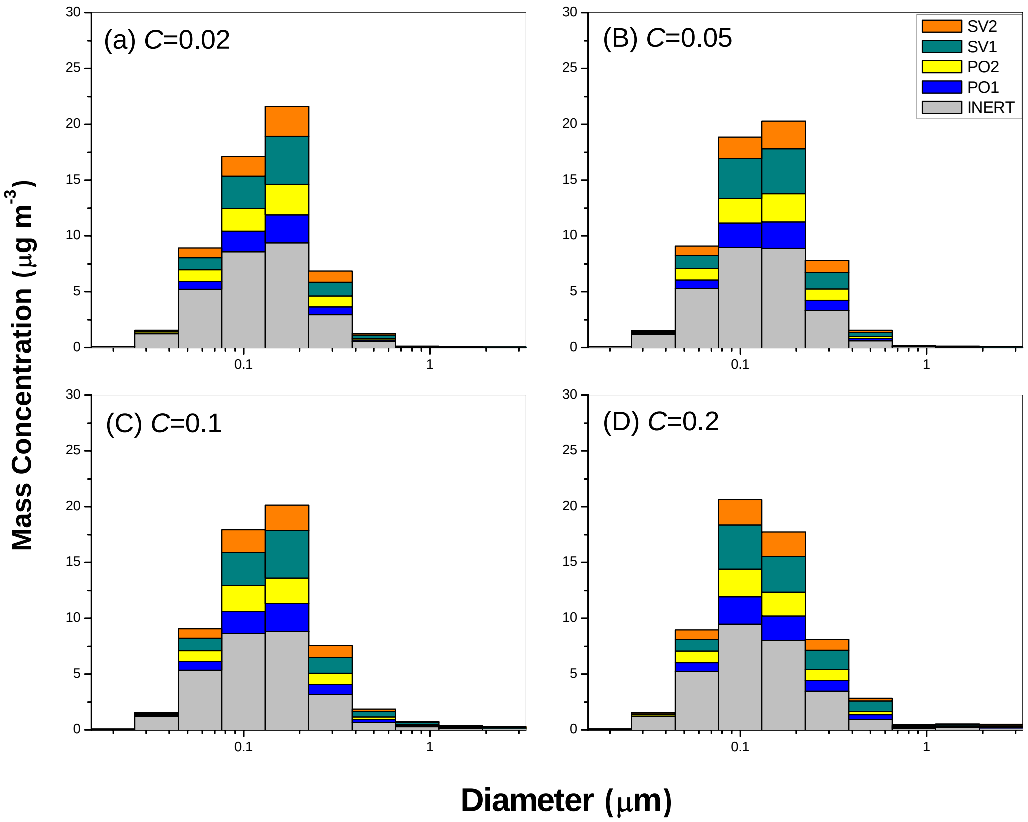

Figure 4.4 Size and components distribution of externally mixed particles with different mixing criteria after 8 days simulation. (a) *c*=0.02, (b) *c*=0.05, (c) *c*=0.1 and (d) *c*=0.2.

Table 4.8 Main distributions* included in externally mixed particles after simulation with different mixing criteria.

Index	Composition					Mass concentration (μg m^{-3})			
	PO1	PO2	SV1	SV2	INERT	0.02	0.05	0.1	0.2
1	+		+			4.328	4.926	5.412	10.925
2		+		+		2.988	3.031	3.368	4.715
3	+	+	+	+		0.915	0.692	0.629	0.053
4					+	12.3	13.451	19.717	37.347
5	+		+		+	8.424	10.448	12.973	1.141
6		+		+	+	7.973	7.871	11.388	0.102
7	+	+	+	+	+	20.372	18.821	4.689	0.000
	Total mass					57.5	59.5	59.5	61.3

* At least 0.5 μg m^{-3} in a section of one distribution.

When the mixing criterion is very small, a small amount of a compound is sufficient to form a mixture, no matter by coagulation or condensation process, leading to a large number of mixture distributions. Some of these distributions only have very small mass and number concentration, but they will significantly increase the computational burden and decrease the calculation speed. Large value of mixing criterion can decrease the number of distributions, thus increasing the simulation speed. But, less number of distributions will distort the component distributions arbitrarily. In Table 4.8, INERT is defined as the only significant compound in distribution 4, though it contains other components with fraction less than threshold. When the mixing criterion is high, large amount of other components is evenly dispersed in distribution 4, which conflicts with the intended definition of externally mixed particles. Thus, a reasonable value is needed for mixing criterion defining.

The definition of mixing criterion, *c*, depends on the mixing system, and is affected by the number and type of compounds considered. For the current simulation system, as shown in Table 4.8 and Figure 4.4, the size and components distributions for mixing threshold of 0.02, 0.05 and 0.1 are much more similar to each other than the distribution with c=0.2. Counting the computation time, 0.05 or 0.1 would be a better mixing criterion choice for current system, which have similar results and need far less time than the criterion of 0.02. For more complex system, where there are tens of components, the value of mixing criterion would be much smaller, in order to consider the effect of all the compounds. Understanding how to define a specific optimum criterion value for different mixing systems is an important topic for future research.

Conclusions

A new Lagrangian aerosol model for SOA formation is built, which includes the partitioning of semivolatile organic compounds (SOCs), coagulation between particles, emission of gas and particles, and deposition processes. In the model, aerosol particles can be defined as external mixture, which is more close to realistic existing status of particles in gas phase, especially for freshly emitted ones. A new definition of externally mixed particles is provided, with the concept of mixing criterion for distinguishing external and internal mixture in aerosol model. And a new coagulation process is formulated, which assigns the coagulated particles to corresponding section and distribution based on their composition and size.

The new model is used for simulations based on a simplified urban scenario, and the results show that the mixing state of externally mixed particles is affected by SOC partitioning and coagulation between particles. Without coagulation, individual SOCs condense preferentially to particles with similar compounds, and thus condensation process increases the difference between particles initially with different components. When there is coagulation, the composition difference between particles is decreased, because of the mixing of particles with different components. All the SOCs can partition to all the particles more easily thereafter, leading to the further decrease of difference between particles. As a result, when modeling aerosol particles as external mixture, coagulation process should not be neglected because it may have a significant influence on particle evolution.

Similarly, the partitioning of SOC is affected by both mixing state and coagulation. When particles are externally mixed, SOC is not evenly distributed to all the particles, which occurs in internal mixture, leading to the different growth rate of particles with different composition. Coagulation between particles decreases the total number of particles, and leads to less SOC condensed to particle phase. The simulation result of external mixture in Table 4.3 clearly shows less condensing of SV1, because some particles (most with PO1) move fast enough to have diameter larger than 1.0 μm, where there is a higher deposition rate and lower surface ratio.

With the sensitivity analysis of mixing criterion for externally mixed particles, the selection of mixing criteria shows limited effects on the final size and compositional distribution of particles, but significant changes on the size and type of individual distributions that compose the external mixture. The definition of mixing criterion depends on the number and type of primary and secondary components in particle phase and the aerosol properties targeted for study. Guidelines for criterion selection for different aerosol systems need to be investigated further.

CHAPTER V

SUMMARY AND CONCLUSIONS

The objective of this research has been to improve the representation of multicomponent aerosol in numerical models, which includes the creation of a method for converting between two different type aerosol distributions, and the construction of an aerosol model for investigating the interactions between aerosol mixing state, SOA partitioning, and coagulation. The new conversion method can accurately convert multicomponent aerosol distributions from sectional to modal representations with the conservation of both total and components mass. The new SOA model can be used to simulate the evolution of both externally and internally mixed particles. The impacts of SOA partitioning on aerosol mixing state and coagulation, coagulation on SOA partitioning and aerosol mixing state, and the aerosol mixing state on SOA partitioning were investigated based on the model.

The new size distribution conversion method uses a non-linear least square regression approach for fitting aerosol sectional distribution with 3 lognormal equations. In tests using an unevenly dispersed 3 component sectional aerosol distribution, results show that the converted modal distribution can accurately represent the original sectional distribution. Compared with other conversion methods, both total and component mass are conserved, the size, shape, and location of peaks match the original distribution, and modal compositions can allocate components to the same size range as in the sectional representation. The new conversion method can also be used even when there are relatively few size sections or where the size sections do not span the entire distribution.

The new aerosol model for SOA formation was used to investigate the interactions between aerosol mixing state, SOA partitioning, and coagulation within a simplified urban scenario with 2 primary, 2 secondary organic components, and 1 inert compound. The trajectory aerosol box model is formulated in a Lagrangian coordinate system, with SOA partitioning, coagulation between particles, emission of organic gases and particles, deposition, and photochemical reactions in gas phase. A new definition of external mixture is provided, with the concept of mixing criterion for distinguishing external and internal mixtures, and the emitted aerosol are treated as externally mixed particles based on this new definition. A new coagulation routine for external mixtures assigns the coagulated particles to corresponding section and distribution based on their composition and size.

Simulation results show that unevenly dispersed components and a broader distribution are produced for externally mixed particles, whereas there is a uniform composition among all the sections in internal mixture. Because of coagulation and condensation, extra distributions other than original ones will be produced for externally mixed particles, leading to the decreased composition difference between particles, and this trend could be accelerated by SOC partitioning. Less SOC may be condensed to particle phase for externally mixed particles, because some distributions will grow to larger sizes and be removed more rapidly due to higher deposition rates. Through sensitivity analysis on the effect of the mixing criterion for external mixture, I found that limited effects were shown for final composition and size distributions, but significant changes occurred for the size and type of individual distributions that compose the external mixture.

In summary, my research has successfully provided a new conversion method and a new aerosol model, both of which can be used to improve the performance of large scale air quality models. Certainly, there is still a lot work to be done for the future implementation in air quality models. Current work has all been done based on theoretical scenarios with many simplified assumptions. The capability and efficiency of these new approaches need to be checked in realistic situations. For conversion method, the realistic atmospheric aerosol has more components, broader distribution, and unclear distribution trend. How to improve the computation efficiency for a complex system and how to fit several indistinct distributions by only 3 modes but still keep the accuracy should be further investigated.

For the new SOA model, future work should include investigations of the difference between externally and internally mixed particles in more complex systems, and the integration and application in air quality models. First, processes that are not included in current model should be added, such as particle nucleation, inorganic compounds in gas and particle phase, interactions between organic and inorganic compounds, and so on. Then differences in component and size distributions between externally and internally mixed particles should be investigated, with a focus on the selection of criterion used for external mixture definition, the standard for grouping multiple similar emission sources and chemical compounds, and methods to improve efficiency and accuracy. Ultimately, the aerosol module should be incorporated into larger air quality models to simulate aerosol behavior more correctly.

REFERENCES

Ackermann, I. J., Hass, H., Memmesheimer, M., Ebel, A., Binkowski, F. S. and Shankar, U. (1998). Modal aerosol dynamics model for Europe: Development and first applications, *Atmospheric Environment* 32(17): 2981-2999.

Atkins, P. W. (1990). *Physical Chemistry*. New York, W. H. Freeman and Company.

Bhave, P. V., Kleeman, M. J., Allen, J. O. and Hughes, L. S. (2002). Evaluation of an air quality model for the size and composition of source-oriented particle classes, *Environmental Science & Technology* 36(10): 2154-2163.

Binkowski, F. S., Ed. (1999). *Aerosols in Models-3 CMAQ*. Science Algorithms of the EPA Models-3 Community Multiscale Air Quality (CMAQ) Modeling Systme. Washington D.C., Office of Rearch And Development, U.S Environmental Protection Agency.

Binkowski, F. S. and Roselle, S. J. (2003). Models-3 community multiscale air quality (CMAQ) model aerosol component - 1. Model description, *Journal of Geophysical Research-Atmospheres* 108(D6).

Binkowski, F. S. and Shankar, U. (1995). The Regional Particulate Matter Model .1. Model description and preliminary results, *Journal of Geophysical Research-Atmospheres* 100(D12): 26191-26209.

Blando, J. D., Porcja, R. J., Li, T. H., Bowman, D., Lioy, P. J. and Turpin, B. J. (1998). Secondary formation and the Smoky Mountain organic aerosol: An examination of aerosol polarity and functional group composition during SEAVS, *Environmental Science & Technology* 32(5): 604-613.

Bowman, F. M. and Karamalegos, A. M. (2002). Estimated effects of composition on secondary organic aerosol mass concentrations, *Environmental Science & Technology* 36(12): 2701-2707.

Bowman, F. M. and Melton, J. A. (2004). Effect of activity coefficient models on predictions of secondary organic aerosol partitioning, *Journal of Aerosol Science* 35(12): 1415-1438.

Bowman, F. M., Odum, J. R., Seinfeld, J. H. and Pandis, S. N. (1997). Mathematical model for gas-particle partitioning of secondary organic aerosols, *Atmospheric Environment* 31(23): 3921-3931.

Brasseur, G. P., Orlando, J. J. and Tyndall, G. S. (1999). *Atmospheric Chemistry and Global Change*. New York, oxford university.

Capaldo, K. P., Pilinis, C. and Pandis, S. N. (2000). A computationally efficient hybrid approach for dynamic gas/aerosol transfer in air quality models, *Atmospheric Environment* 34(21): 3617-3627.

Carter, W. P. L. (1990). A Detailed Mechanism for the Gas-Phase Atmospheric Reactions of Organic-Compounds, *Atmospheric Environment Part a-General Topics* 24(3): 481-518.

Chandramouli, B., Jang, M. and Kamens, R. M. (2003a). Gas-particle partitioning of semi-volatile organics on organic aerosols using a predictive activity coefficient model: analysis of the effects of parameter choices on model performance, *Atmospheric Environment* 37(6): 853-864.

Chandramouli, B., Jang, M. S. and Kamens, R. M. (2003b). Gas-particle partitioning of semivolatile organic compounds (SOCs) on mixtures of aerosols in a smog chamber, *Environmental Science & Technology* 37(18): 4113-4121.

Douglas, S. (2002). *Experience in PM2.5 modeling of the southeastern u.s.*, VISTAS Technical Workgroup. http://www.vistas-sesarm.org/tech/workshop1002_douglas_pm_modeling.pdf. San Francisco, CA.

FassiFihri, A., Suhre, K. and Rosset, R. (1997). Internal and external mixing in atmospheric aerosols by coagulation: Impact on the optical and hygroscopic properties of the sulphate-soot system, *Atmospheric Environment* 31(10): 1393-1402.

Fitzgerald, J. W., Hoppel, W. A. and Gelbard, F. (1998). A one-dimensional sectional model to simulate multicomponent aerosol dynamics in the marine boundary layer - 1. Model description, *Journal of Geophysical Research-Atmospheres* 103(D13): 16085-16102.

Fredenslund, A., Jones, R. L. and Prausnitz, J. M. (1975). Group-Contribution Estimation of Activity-Coefficients in Nonideal Liquid-Mixtures, *Aiche Journal* 21(6): 1086-1099.

Gard, E. E., Kleeman, M. J., Gross, D. S., Hughes, L. S., Allen, J. O., Morrical, B. D., Fergenson, D. P., Dienes, T., Galli, M. E., Johnson, R. J., Cass, G. R. and Prather, K. A. (1998). Direct observation of heterogeneous chemistry in the atmosphere, *Science* 279(5354): 1184-1187.

Gelbard, F. (1990). Modeling Multicomponent Aerosol-Particle Growth by Vapor Condensation, *Aerosol Science and Technology* 12(2): 399-412.

Gelbard, F. and Seinfeld, J. H. (1980). Simulation of Multicomponent Aerosol Dynamics, *Journal of Colloid and Interface Science* 78(2): 485-501.

Gelbard, F., Tambour, Y. and Seinfeld, J. H. (1980). Sectional Representations for Simulating Aerosol Dynamics, *Journal of Colloid and Interface Science* 76(2): 541-556.

Griffin, R. J., Cocker, D. R., Flagan, R. C. and Seinfeld, J. H. (1999). Organic aerosol formation from the oxidation of biogenic hydrocarbons, *Journal of Geophysical Research-Atmospheres* 104(D3): 3555-3567.

Griffin, R. J., Dabdub, D., Kleeman, M. J., Fraser, M. P., Cass, G. R. and Seinfeld, J. H. (2002a). Secondary organic aerosol - 3. Urban/regional scale model of size- and composition-resolved aerosols, *Journal of Geophysical Research-Atmospheres* 107(D17): -.

Griffin, R. J., Dabdub, D. and Seinfeld, J. H. (2002b). Secondary organic aerosol - 1. Atmospheric chemical mechanism for production of molecular constituents, *Journal of Geophysical Research-Atmospheres* 107(D17): -.

Harrington, D. Y. and Kreidenweis, S. M. (1998). Simulations of sulfate aerosol dynamics - Part II. Model intercomparison, *Atmospheric Environment* 32(10): 1701-1709.

Hasegawa, S. and Ohta, S. (2002). Some measurements of the mixing state of soot-containing particles at urban and non-urban sites, *Atmospheric Environment* 36: 3899-3908.

Held, T., Ying, Q., Kaduwela, A. and Kleeman, M. (2004). Modeling particulate matter in the San Joaquin Valley with a source-oriented externally mixed three-dimensional photochemical grid model, *Atmospheric Environment* 38(22): 3689-3711.

Hildemann, L. M., Markowski, G. R. and Cass, G. R. (1991). Chemical-Composition of Emissions from Urban Sources of Fine Organic Aerosol, *Environmental Science & Technology* 25(4): 744-759.

Hinds, W. C. (1999). *Aerosol Technology: Properties, Behavior, and Measurement of Airborne Particles*, John Wiley.

Jacobson, M. and Seinfeld, J. H. (2004). Evolution of nanoparticle size and mixing state near the point of emission, *Atmospheric Environment* 38: 1839 - 1850.

Jacobson, M. C., Hansson, H. C., Noone, K. J. and Charlson, R. J. (2000). Organic atmospheric aerosols: Review and state of the science, *Reviews of Geophysics* 38(2): 267-294.

Jacobson, M. Z. (1997a). Development and application of a new air pollution modeling system .2. Aerosol module structure and design, *Atmospheric Environment* 31(2): 131-144.

Jacobson, M. Z. (1997b). Development and application of a new air pollution modeling system .3. Aerosol-phase simulations, *Atmospheric Environment* 31(4): 587-608.

Jacobson, M. Z. (1997c). *Fundamentals of Atmospheric Modeling*. New York, Cambridge University.

Jacobson, M. Z. (2001a). GATOR-GCMM: A global- through urban-scale air pollution and weather forecast model 1. Model design and treatment of subgrid soil, vegetation, roads, rooftops, water, sea ice, and snow, *Journal of Geophysical Research-Atmospheres* 106(D6): 5385-5401.

Jacobson, M. Z. (2001b). Strong radiative heating due to the mixing state of black carbon in atmospheric aerosols, *Nature* 409(6821): 695-697.

Jacobson, M. Z. (2002). Analysis of aerosol interactions with numerical techniques for solving coagulation, nucleation, condensation, dissolution, and reversible chemistry among multiple size distributions, *Journal of Geophysical Research-Atmospheres* 107(D19).

Jacobson, M. Z., Turco, R. P., Jensen, E. J. and Toon, O. B. (1994). Modeling Coagulation among Particles of Different Composition and Size, *Atmospheric Environment* 28(7): 1327-1338.

Kleeman, M. J. and Cass, G. R. (2001). A 3D Eulerian source-oriented model for an externally mixed aerosol, *Environmental Science & Technology* 35(24): 4834-4848.

Kleeman, M. J., Cass, G. R. and Eldering, A. (1997). Modeling the airborne particle complex as a source-oriented external mixture, *Journal of Geophysical Research-Atmospheres* 102(D17): 21355-21372.

Kleeman, M. J., Hughes, L. S., Allen, J. O. and Cass, G. R. (1999). Source contributions to the size and composition distribution of atmospheric particles: Southern California in September 1996, *Environmental Science & Technology* 33(23): 4331-4341.

Koo, B. Y., Ansari, A. S. and Pandis, S. N. (2003). Integrated approaches to modeling the organic and inorganic atmospheric aerosol components, *Atmospheric Environment* 37(34): 4757-4768.

Lawson, D. R. (1990). The Southern California Air-Quality Study, *Journal of the Air & Waste Management Association* 40(2): 156-165.

Leach, K. B., Kamens, R. M., Strommen, M. R. and Jang, M. (1999). Partitioning of semivolatile organic compounds in the presence of a secondary organic aerosol in a controlled atmosphere, *Journal of Atmospheric Chemistry* 33(3): 241-264.

Lee, K. W. (1983). Change of Particle-Size Distribution During Brownian Coagulation, *Journal of Colloid and Interface Science* 92(2): 315-325.

Liang, C. K., Pankow, J. F., Odum, J. R. and Seinfeld, J. H. (1997). Gas/particle partitioning of semivolatile organic compounds to model inorganic, organic, and ambient smog aerosols, *Environmental Science & Technology* 31(11): 3086-3092.

Lurmann, F. W., Wexler, A. S., Pandis, S. N., Musarra, S., Kumar, N. and Seinfeld, J. H. (1997). Modelling urban and regional aerosols .2. Application to California's South Coast Air Basin, *Atmospheric Environment* 31(17): 2695-2715.

Malm, W. C. and Day, D. E. (2000). Optical properties of aerosols at Grand Canyon National Park, *Atmospheric Environment* 34(20): 3373-3391.

Malm, W. C., Day, D. E., Kreidenweis, S. M., Collett, J. L. and Lee, T. (2003). Humidity-dependent optical properties of fine particles during the Big Bend regional aerosol and visibility observational study, *Journal of Geophysical Research-Atmospheres* 108(D9): -.

Mebust, M. R., Eder, B. K., Binkowski, F. S. and Roselle, S. J. (2003). Models-3 community multiscale air quality (CMAQ) model aerosol component - 2. Model evaluation, *Journal of Geophysical Research-Atmospheres* 108(D6).

Meng, Z. Y., Dabdub, D. and Seinfeld, J. H. (1998). Size-resolved and chemically resolved model of atmospheric aerosol dynamics, *Journal of Geophysical Research-Atmospheres* 103(D3): 3419-3435.

Meng, Z. Y. and Seinfeld, J. H. (1996). Time scales to achieve atmospheric gas-aerosol equilibrium for volatile species, *Atmospheric Environment* 30(16): 2889-2900.

More, J. J., Garbow, B. S. and Hillstrom, K. E. (1980). *Implementation guide for MINPACK-1*. Technical Report ANL-80-68, Mathematics and Computer Sciences Division, Argonne National Laboratory. Argonne, IL.

Moya, M., Pandis, S. N. and Jacobson, M. Z. (2002). Is the size distribution of urban aerosols determined by thermodynamic equilibrium? An application to Southern California, *Atmospheric Environment* 36(14): 2349-2365.

Mysliwiec, M. J. and Kleeman, M. J. (2002). Source apportionment of secondary airborne particulate matter in a polluted atmospbere, *Environmental Science & Technology* 36(24): 5376-5384.

Naoe, H. and Okada, K. (2001). Mixing properties of submicrometer aerosol particles in the urban atmosphere - with regard to soot particles, *Atmospheric Environment* 35(33): 5765-5772.

Noble, C. A. and Prather, K. A. (1996). Real-time measurement of correlated size and composition profiles of individual atmospheric aerosol particles, *Environmental Science & Technology* 30(9): 2667-2680.

Odum, J. R., Hoffmann, T., Bowman, F., Collins, D., Flagan, R. C. and Seinfeld, J. H. (1996). Gas/particle partitioning and secondary organic aerosol yields, *Environmental Science & Technology* 30(8): 2580-2585.

Pandis, S. N., Harley, R. A., Cass, G. R. and Seinfeld, J. H. (1992). Secondary Organic Aerosol Formation and Transport, *Atmospheric Environment Part a-General Topics* 26(13): 2269-2282.

Pankow, J. F. (1994). An Absorption-Model of Gas-Particle Partitioning of Organic-Compounds in the Atmosphere, *Atmospheric Environment* 28(2): 185-188.

Pankow, J. F., Seinfeld, J. H., Asher, W. E. and Erdakos, G. B. (2001). Modeling the formation of secondary organic aerosol. 1. Application of theoretical principles to measurements obtained in the alpha-pinene/, beta- pinene/, sabinene/, Delta(3)-carene/, and cyclohexene/ozone systems, *Environmental Science & Technology* 35(6): 1164-1172.

Penner, J. E., Andreae, M., Annegarn, H., Barrie, L., Feichter, J., Hegg, D., Jayaraman, A., Leaitch, R., Murphy, D., Nganga, J. and Pitari, G. (2001). *Aerosols, their Direct and Indirect Effects, in Climate Change 2001: The Scientific Basis*. Cambridge, UK, Cambridge University Press.

Phalen, R. F. (1998). Uncertainties relating to the health effects of particulate air pollution: The US EPA's particle standard, *Toxicology Letters* 96-7: 263-267.

Pilinis, C., Capaldo, K. P., Nenes, A. and Pandis, S. N. (2000). MADM - A new multicomponent aerosol dynamics model, *Aerosol Science and Technology* 32(5): 482-502.

Pope, C. A. (2000). Review: Epidemiological basis for particulate air pollution health standards, *Aerosol Science and Technology* 32(1): 4-14.

Pun, B. K., Griffin, R. J., Seigneur, C. and Seinfeld, J. H. (2002). Secondary organic aerosol - 2. Thermodynamic model for gas/particle partitioning of molecular constituents, *Journal of Geophysical Research-Atmospheres* 107(D17): -.

Rogge, W. F., Hildemann, L. M., Mazurek, M. A., Cass, G. R. and Simoneit, B. R. T. (1993). Sources of Fine Organic Aerosol .2. Noncatalyst and Catalyst-Equipped Automobiles and Heavy-Duty Diesel Trucks, *Environmental Science & Technology* 27(4): 636-651.

Russell, L. M. and Seinfeld, J. H. (1998). Size- and composition-resolved externally mixed aerosol model, *Aerosol Science and Technology* 28(5): 403-416.

Seigneur, C. (2001). Current status of air quality models for particulate matter, *Journal of the Air & Waste Management Association* 51(11): 1508-1521.

Seigneur, C., Hudischewskyj, A. B., Seinfeld, J. H., Whitby, K. T., Whitby, E. R., Brock, J. R. and Barnes, H. M. (1986). Simulation of Aerosol Dynamics - a Comparative Review of Mathematical-Models, *Aerosol Science and Technology* 5(2): 205-222.

Seinfeld, J. H. and Pandis, S. N. (1998). *Atmospheric Chemistry and Physics: From Air Pollution to Global Change*. New York, John Wiley.

Sheehan, P. E. and Bowman, F. M. (2001). Estimated effects of temperature on secondary organic aerosol concentrations, *Environmental Science & Technology* 35(11): 2129-2135.

Solomon, P. A., Chameides, W., Weber, R., Middlebrook, A., Kiang, C. S., Russell, A. G., Butler, A., Turpin, B., Mikel, D., Scheffe, R., Cowling, E., Edgerton, E., St John, J., Jansen, J., McMurry, P., Hering, S. and Bahadori, T. (2003). Overview of the 1999 Atlanta Supersite Project, *Journal of Geophysical Research-Atmospheres* 108(D7): -.

Sun, Q. and Wexler, A. S. (1998a). Modeling urban and regional aerosols - Condensation and evaporation near acid neutrality, *Atmospheric Environment* 32(20): 3527-3531.

Sun, Q. and Wexler, A. S. (1998b). Modeling urban and regional aerosols near acid neutrality - Application to the 24-25 June SCAQS episode, *Atmospheric Environment* 32(20): 3533-3545.

Sun, Z., Axelbaum, R. L. and Huertas, J. I. (2004). Monte Carlo simulation of multicomponent aerosols undergoing simultaneous coagulation and condensation, *Aerosol Science and Technology* 38(10): 963-971.

Trautmann, T. and Wanner, C. (1999). A fast and efficient modified sectional method for simulating multicomponent collisional kinetics, *Atmospheric Environment* 33(10): 1631-1640.

Turpin, B. J., Saxena, P. and Andrews, E. (2000). Measuring and simulating particulate organics in the atmosphere: problems and prospects, *Atmospheric Environment* 34(18): 2983-3013.

Venkatram, A., Karamchandani, P., Pai, P., Sloane, C., Saxena, P. and Goldstein, R. (1997). The development of a model to examine source-receptor relationships for visibility on the Colorado Plateau, *Journal of the Air & Waste Management Association* 47(3): 286-301.

Vignati, E., Berkowicz, R., Palmgren, F., Lyck, E. and Hummelshoj, F. (1999). Transformation of size distributions of emitted particles in streets, *Science of the Total Environment* 235(1-3): 37-49.

Warren, D. R. and Seinfeld, J. H. (1985). Simulation of Aerosol Size Distribution Evolution in Systems with Simultaneous Nucleation, Condensation, and Coagulation, *Aerosol Science and Technology* 4(1): 31-43.

Wexler, A. S., Lurmann, F. W. and Seinfeld, J. H. (1994). Modeling Urban and Regional Aerosols .1. Model Development, *Atmospheric Environment* 28(3): 531-546.

Wexler, A. S. and Seinfeld, J. H. (1990). The Distribution of Ammonium-Salts among a Size and Composition Dispersed Aerosol, *Atmospheric Environment Part a-General Topics* 24(5): 1231-1246.

Whitby, E., Stratmann, F. and Wilck, M. (2002). Merging and remapping modes in modal aerosol dynamics models: a "Dynamic Mode Manager", *Journal of Aerosol Science* 33(4): 623-645.

Whitby, E. R. and McMurry, P. H. (1997). Modal aerosol dynamics modeling, *Aerosol Science and Technology* 27(6): 673-688.

Whitby, K. T. (1978). Physical Characteristics of Sulfur Aerosols, *Atmospheric Environment* 12(1-3): 135-159.

Wilck, M. and Stratmann, F. (1997). A 2-D multicomponent modal aerosol model and its application to laminar flow reactors, *Journal of Aerosol Science* 28(6): 959-972.

Ying, Q., Mysliwiec, M. and Kleeman, M. J. (2004). Source apportionment of visibility impairment using a three-dimensional source-oriented air quality model, *Environmental Science & Technology* 38(4): 1089-1101.

Yong, P. K. and Seinfeld, J. H. (1992). Simulation of Multicomponent Aerosol Dynamics, *Journal of Colloid and Interface Science* 149(2): 425-449.

Zhang, Y., Easter, R. C., Ghan, S. J. and Abdul-Razzak, H. (2002). Impact of aerosol size representation on modeling aerosol-cloud interactions, *Journal of Geophysical Research-Atmospheres* 107(D21): -.

Zhang, Y., Pun, B., Vijayaraghavan, K., Wu, S. Y., Seigneur, C., Pandis, S. N., Jacobson, M. Z., Nenes, A. and Seinfeld, J. H. (2004). Development and application of the model of aerosol dynamics, reaction, ionization, and dissolution (MADRID), *Journal of Geophysical Research-Atmospheres* 109(D1).

Zhang, Y., Seigneur, C., Seinfeld, J. H., Jacobson, M., Clegg, S. L. and Binkowski, F. S. (2000). A comparative review of inorganic aerosol thermodynamic equilibrium modules: similarities, differences, and their likely causes, *Atmospheric Environment* 34(1): 117-137.